# HÖGANÄS HANDBOOK FOR WARM COMPACTION

Höganäs

## Foreword

The purpose of this book is to explain the major possibilities created in powder metallurgy by warm compaction technology, as compared with conventional 'cold' compaction. In the first instance, the book is intended for those who have some experience of iron powder technologies and are considering moving into warm compaction. Consequently, this is a basic guide which contains far from all the details needed to establish and operate a warm compaction plant. Included here, however, are definitive, general principles and guidelines for applying warm compaction appropriately.

Presented first is a general description of the warm compaction process, followed by a more detailed study of various aspects of the method. In chapter 10 a practical guide with corrective responses for optimal operations is presented, based on experiences with installation, starting up and operating of warm compaction tools. Finally, the book includes a list of useful references and a collection of photographs of the essential components of the process.

Höganäs AB
2004

# Table of contents

# 1 Introduction

The production of solid components from metal powders by compaction and sintering is known as powder metallurgy (P/M). Efforts to improve P/M technology have focused on ways to enhance the mechanical properties and tolerances of finished parts, in order to expand the market and give lowest total cost overall. There are two main ways:

1. Control and modify metallic micro structure, and/or,
2. Control and modify pore micro structure.

A major advance in P/M technology has been the warm compaction process which produces changes in the pore morphology of sintered parts, compared to that obtained with conventional 'cold' compaction. The result is that higher density levels are achieved and, at the same time, warm compaction products have more even density distributions (i.e. less variation in density within a component). The warm compaction process is applicable to most powder/material systems. This will lead to higher strength and better dimensional tolerances. A possibility of green machining is also obtained by this process partly due to high green strength.

This handbook presents both theoretical aspects of warm compaction and practical experiences, and guidelines to obtain good process control and desired properties.

## 2 Warm compaction process

The warm compaction process, outlined below, utilizes traditional powder metallurgy compaction equipment and is applicable to most powder/material systems but requires that both the powder and the die assembly are heated to temperatures in the range of 100-150°C. See figure 1.

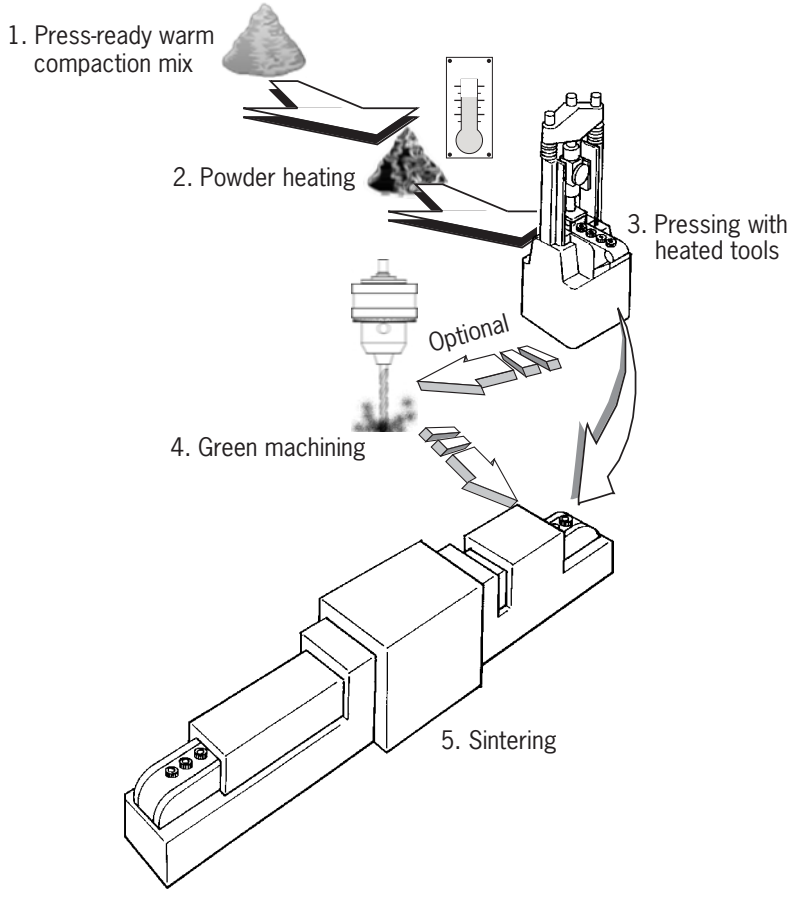


*Figure 1. Schematic outline of the warm compaction process.*

How then, is warm compaction to be defined? Temperature limits for working with warm compaction are set according to the demands of current materials technology. Above 150°C lubricants begin to break down, and at these higher temperatures iron powders oxidize more rapidly. At temperatures below about 100°C sufficient compaction effect cannot be achieved. Therefore the range 100-150°C roughly delimits the working temperatures which currently define warm compaction.

It is possible that in the foreseeable future advances in powder technology will allow for compaction at higher temperatures, and that even greater densities may be reliably produced. To reach this goal however, a whole new powder technology may be needed.

Which specific temperature is aimed at depends on the powder technology used. Höganäs AB supplies Densmix™ where the powder temperature can be between 125-130°C and the tool temperature between 130-150°C. Chapter 4, "Process Robustness", deals more in detail with these questions. In order to heat the powder three different technologies exist today:

**1. Slot Heater**
Slot Heater uses a conventional heat exchanger with oil-heated elements, where the powder is free flowing to the filling shoe and the die.

**2. EL-temp**
EL-temp utilizes a heated screw feeder (an auger) which together with heating the powder, transports it to the filling shoe.

**3. Abbot**
Abbot transfers heat to the powder with a fluidised bed.

Along with the powder heating warm compaction requires heating of the die assembly. It means usually that: the powder transport hoses to the filling shoe (if any), filling shoe, upper punch, die, and adaptor table must all be heated. Specific guidelines are presented in following sections.

# 3 Theory

This section presents a model to understand the higher densities, and more even density distribution, achieved with warm compaction compared to conventional "cold"compaction. The model focuses on the effect of yielding in the radial and axial stresses during uni-axial pressing.
When the piston of a hydraulic cylinder exerts pressure upon the liquid inside the cylinder, the pressure applied in axial direction is transformed 1:1 to radial pressure upon the cylinder wall. When a powder is being compacted in a rigid cylindrical die, the axial pressure, exerted upon the powder by the compacting punch, is only partly transformed to radial pressure upon the die wall.

This radial pressure can be quite substantial, but it cannot reach the level of the axial pressure because a powder is not liquid and has no hydraulic properties.

## 3.1 Hysteresis of the Radial Pressure

The way in which the empirical relationship between radial and axial pressure is governed by general laws of physics and mechanics can be understood, in principle at least, from a simple model, suggested in 1960 by W.M. Long[1], and presented in detail below. First, we consider a free-standing cylindrical plug of metal having a modulus of elasticity E and a Poisson factor $\nu$. A compressive axial stress $\sigma_a$, applied to the end-faces of the plug, provokes by laws of elasticity, a radial stress $\sigma_r$ , and the radius of the plug is expanded by the factor

$$\varepsilon_r = (\sigma_r - \nu\sigma_r - \nu\sigma_a)/E \qquad (1)$$

We now imagine the same plug being put into a tightly fitting cylindrical die. The die is assumed to have a modulus of elasticity much larger than that of the metal plug. Further, it is assumed that the die is extremely well lubricated, such that any friction between the plug and the die-wall is negligible. Exerting, via two counteracting punches, axial pressure upon the plug, its radial expansion $\varepsilon_r$ is negligibly small because the die expands extremely little due to its large modulus of elasticity. Thus, $\varepsilon_r = 0$ is a sufficiently close approximation of reality, and from (1), it follows:

$$\sigma_r - \nu\sigma_r - \nu\sigma_a = 0 \qquad (2)$$

Hence, the relationship between radial and axial stress in the plug is:

$$\sigma_r = \sigma_a\nu/(1 - \nu), \text{ elastic loading} \qquad (3)$$

[1] W.M. Long, Powder Metallurgy, No. 6, 1960.

The maximum shearing-stress in the plug (derived from Mohr's circle) is always :

$$\tau_{max} = (\sigma_a - \sigma_r) / 2 \quad (4)$$

With increasing axial stress in the plug, $\tau_{max}$ increases too, until it exceeds the shearing yield-stress $\tau_0 = \sigma_0 /2$, i.e. until $\tau_{max} \geq \sigma_0 / 2$ . Then, from (4), the following condition of flow emerges:

$$(\sigma_a - \sigma_r) \geq \sigma_0 \text{ , } (\sigma_0 = \text{yield point of the metal plug}). \quad (5)$$

Now, plastic flow occurs in the plug, and the relationship between radial and axial stress in the plug is:

$$\sigma_r = \sigma_a - \sigma_0, \textbf{ plastic loading} \quad (6)$$

At axial pressure release, $\tau_{max}$ immediately falls below the level of the shearing yield-stress ($\tau_{max} < \sigma_0 /2$), and the stresses in the metal plug are being released according to:

$$\sigma_r = \sigma_a \nu/(1 - \nu) + k, \textbf{ elastic releasing } (k = \text{constant}) \quad (7)$$

In the course of continued release, the axial stress in the plug decreases and eventually becomes even smaller than the radial stress. From this point on, the following condition of flow rules:

$$(\sigma_r - \sigma_a) \geq \sigma_0 \quad (8)$$

and the relationship between radial and axial stress is:

$$\sigma_r = \sigma_a + \sigma_0, \textbf{ plastic releasing} \quad (9)$$

From the above description, it is evident that the entire loading-releasing cycle, which the metal plug undergoes in the compacting die, forms a hysteresis.
See figure 2 on page 11.

A particularly interesting detail of this hysteresis is the fact that, after complete release of the axial stress, the plug remains under a compressive radial stress $\sigma_r$ which is equal to the metals yield point $\sigma_0$. In this respect, Long's model provides a plausible explanation of the spring-back effect occurring when powder compacts are ejected from the compacting die.

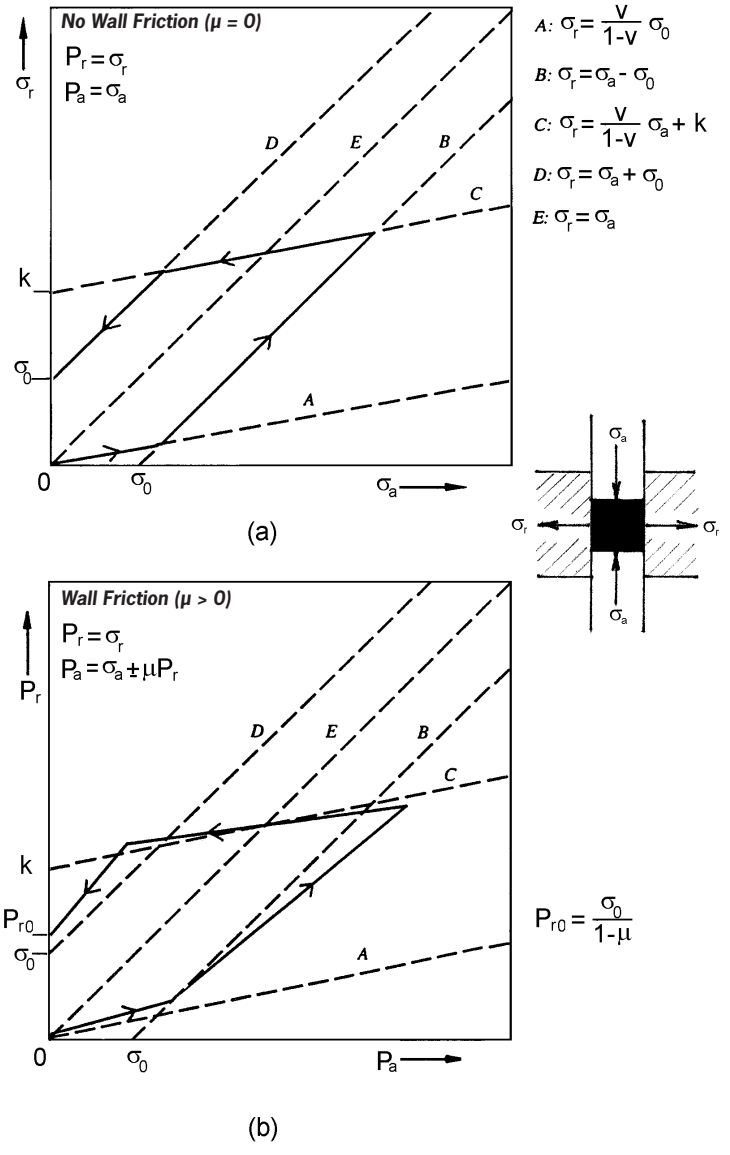


*Figure 2. Relationship between radial and axial pressure occurring in a cylindrical metal plug inside a rigid die during a cycle of loading and releasing the axial pressure. (a) Theoretical model disregarding die-wall friction [7]. (b) Theoretical model including the aspect of die-wall friction [8].*

Although Long's model oversimplifies reality in several respects (absence of wall friction, and deformation strengthening), it provides, along general lines, a fairly satisfactory description of the actual relationship between radial and axial pressure occurring when metal powder is being compacted in a rigid die.

Experimental proof of the hysteresis curve predicted by Long's model has been given for several materials by Long himself as well as by other authors. A modified model, suggested by G. Bockstiegel [2], includes the aspect of die-wall friction as briefly described below. The frictional forces, occurring at the die wall during powder compaction, act in a direction opposite to the movement of the compacting punch. Thus, while the punch moves inward, the compressive axial stress in the powder $\sigma_a$ is smaller than the external punch pressure $P_a$, and while the punch moves outward, $\sigma_a$ is larger than $P_a$. It can be assumed that the frictional force at the die wall is approximately proportional to the radial pressure $P_r$ acting upon the die wall. Hence, the following statement is made:

$$\sigma_a = P_a \pm \mu P_r \qquad (10)$$

The negative sign refers to the phase of pressure increase, the positive sign to the phase of pressure release. $\mu$ is the frictional coefficient residing at the die wall. The radial pressure upon the die wall $P_r$ is identical with the radial stress in the powder, i.e. $P_r = \sigma_r$.

Introducing (10) into Long's equations (3), (6), (7) and (9), these are transformed into corresponding equations pertaining to the modified model:

$$P_r = P_a \nu/(1 - \nu - \mu\nu), \text{ elastic loading} \qquad (3')$$

$$P_r = (P_a - \sigma_0)/(1 + \mu), \text{ plastic loading} \qquad (6')$$

$$P_r = P_a \nu/(1 - \nu + \mu\nu) + k', \text{ elastic releasing, } (k' = \text{constant}) \qquad (7')$$

$$P_r = (P_a + \sigma_0)/(1 - \mu), \text{ plastic releasing} \qquad (9')$$

For $\mu = 0$ (no wall friction), the modified equations ( ' ) are identical with Long's original equations ( ). Although the modified model is based on a statement which rather simplifies the real conditions of stress and friction at the die wall, it makes evident that the inclusion of wall friction does not change Long's model in its general outlines.

[2] G. Bockstiegel, Höganäs 1967

The hysteresis curve of the loading-releasing cycle is merely being somewhat distorted. See figure 2.

During the densification of metal powders, the powder mass does not suddenly switch from elastic to plastic behavior as suggested by Long's model, but the transition occurs gradually in the individual powder particles. Apart from this difference, deformation strengthening occurs in the powder particles during densification.

Corresponding to these circumstances, the slope of experimental hysteresis curves changes gradually with increasing pressure instead of suddenly. See figure 3.

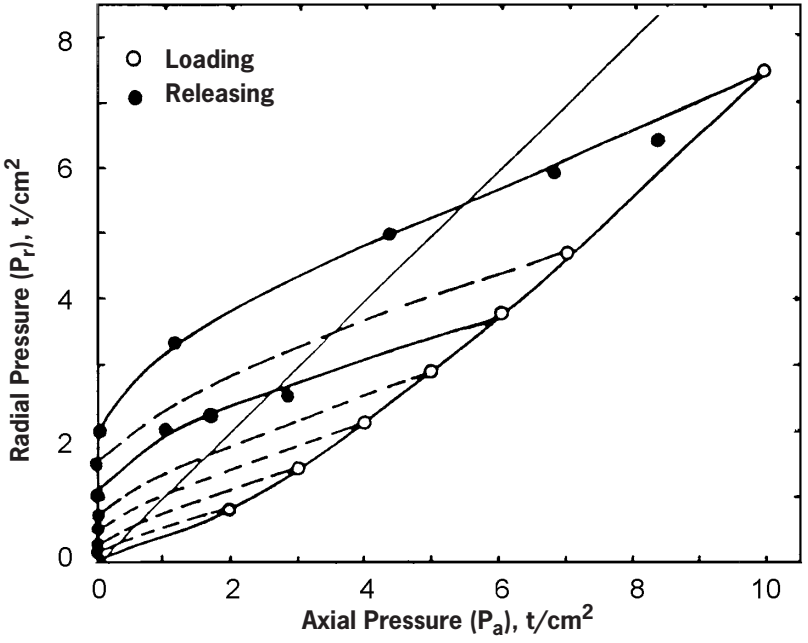


*Figure 3. Radial and axial pressures measured on compacts of sponge iron powder during a loading-releasing cycle in a cylindrical die [9].*

## 3.2 Influence of the Yield Point

From Long's model, it is evident that the radial pressure, which a metal plug or a mass of metal powder under axial pressure exerts upon the wall of a compacting die, is in inverse proportion to yield point of the metal. That is, the smaller the radial pressure, the higher the yield point of a metal. Vice versa, from the same model, it can be concluded that a metal powder with extremely low yield point and negligible tendency to deformation strengthening, like lead powder for instance, should exhibit a nearly hydraulic behavior when compacted in a rigid die. Experimental proof is shown in the diagram. See figure 4.

The entire loading-releasing cycle for lead powder does not show any hysteresis, and its very slight deviation from the ideal hydraulic straight line is due to frictional forces at the die wall.

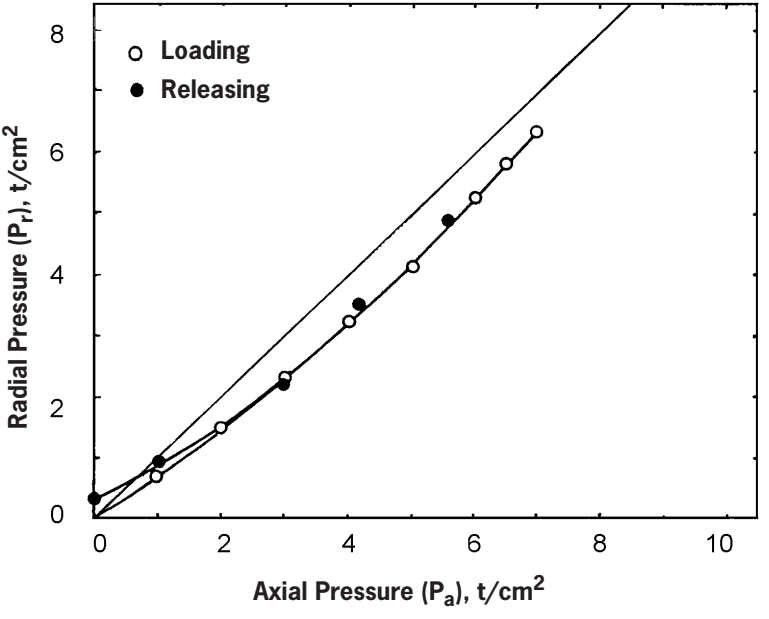


*Figure 4. Radial and axial pressures measured on compacts of lead powder during a loading releasing cycle in a cylindrical die. [9].*

These findings suggest that higher and more homogeneous densities in metal powder compacts could be achieved, if the compacting procedure was executed at elevated temperatures where the yield point of the metal is lower than at R.T.

The principle influence of a temperature-dependent yield point on the relationship between axial and radial pressure emerges from the theoretical hysteresis curves. See figure 5. From these curves, it can be seen that the maximum radial pressure increases but the residual radial pressure, after complete release of the axial pressure, decreases when the yield point is lowered at elevated temperatures.

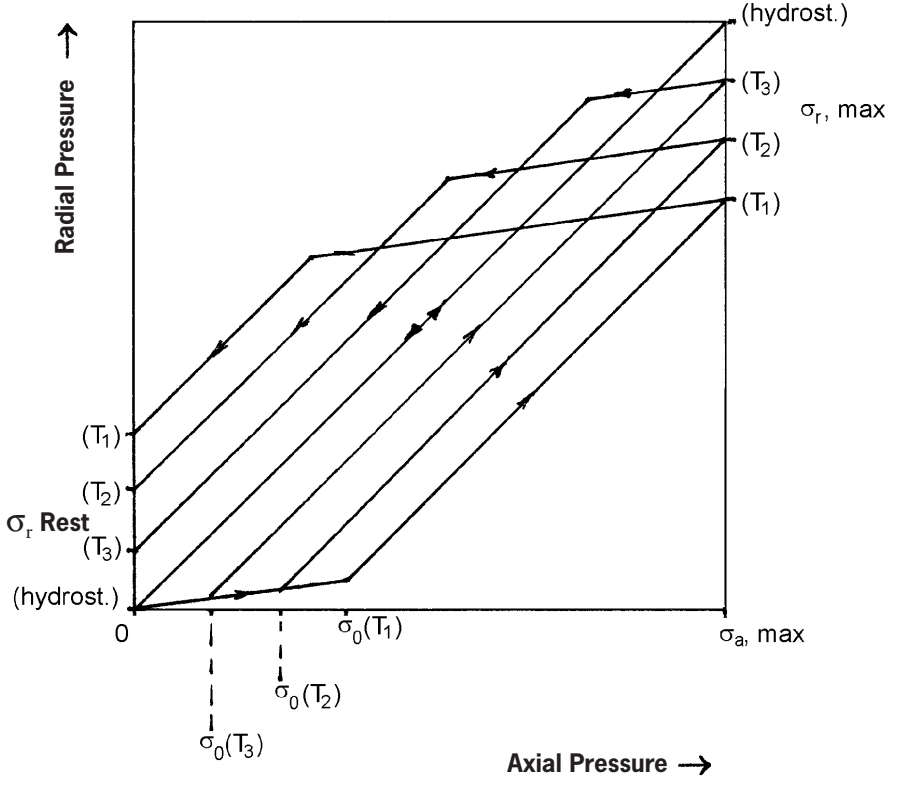


*Figure 5. Influence of the yield point $\sigma_0$ on the relationship between radial and axial pressure for a metal plug inside a cylindrical die during a loading-releasing cycle.*
*Example: the yield point $\sigma_0$ (T) decreases with increasing temperature T ($T_3 > T_2 > T_1$). [10].*

### 3.3 Temperature Influence on Yield Point

There is a significant influence of temperature on deformation behaviour. Deformation of metals can be looked upon as a thermally activated process [12], where both the elastic, reversible, and the plastic, irreversible, deformation is affected.

The microscopical mechanisms that explain this behaviour are complex and in some cases not yet revealed, but the trend is nevertheless there; higher temperature gives lower deformation resistance (in this case quantified by the yield strength). Below there is an example of this behaviour. See figure 6.

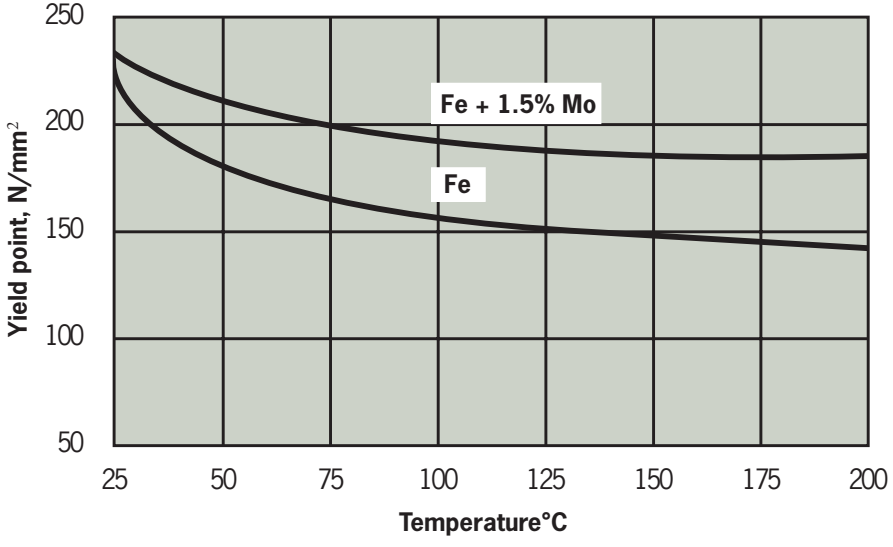


*Figure 6. Influence of temperature on yield point of Fe and Fe + 1.5% Mo. Forged cylinders in compression test at a compression rate of 0.5/s.*

# 4 Process Robustness

To obtain high productivity and close tolerances when using warm compaction in production of parts it is necessary that the powder mix fulfils the same requirements as in conventional compaction at room temperature, i.e. consistent apparent density and flowability. Densmix™ contains a lubricant system developed to give good flowability and filling behaviour at increased temperatures. See figure 7.

It can be seen that both apparent density and flow of the powder are very stable and not sensitive to temperature variations up to 135°C. However at further increased temperatures these properties are changed so that the apparent density is decreased and the flow rate increases, i.e the filling behaviour of the powder becomes worse resulting in an increased scatter of weight and tolerances of the compacted parts.

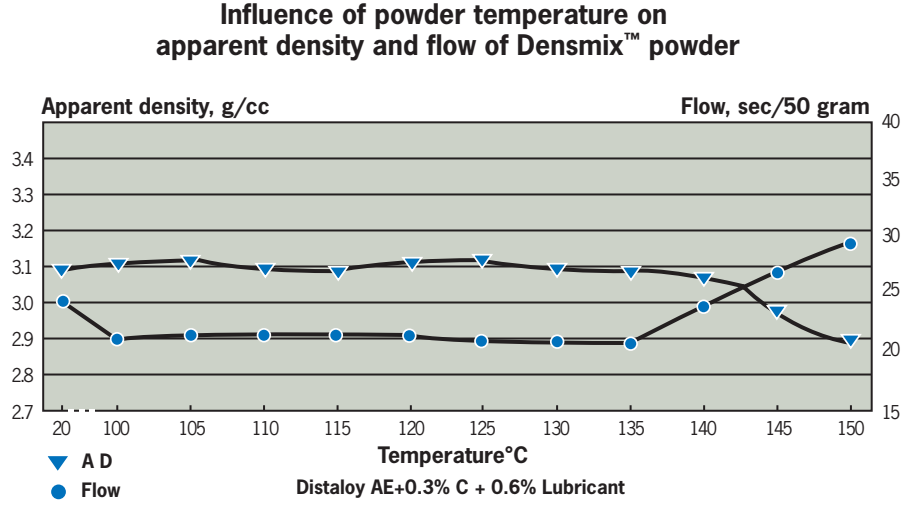


*Figure 7. Influence of powder temperature on apparent density and flow. (The measurements were made by a Hall Flow-meter at different temperatures).*

The weight scatter as a function of powder temperature is presented in the next figure which confirms the results from figure 3. Data were generated from compacting 1000 rings (outer diameter=35 mm, inner diameter=25mm) in an automatic 45 ton Dorst press at different powder temperatures. See figure 8.

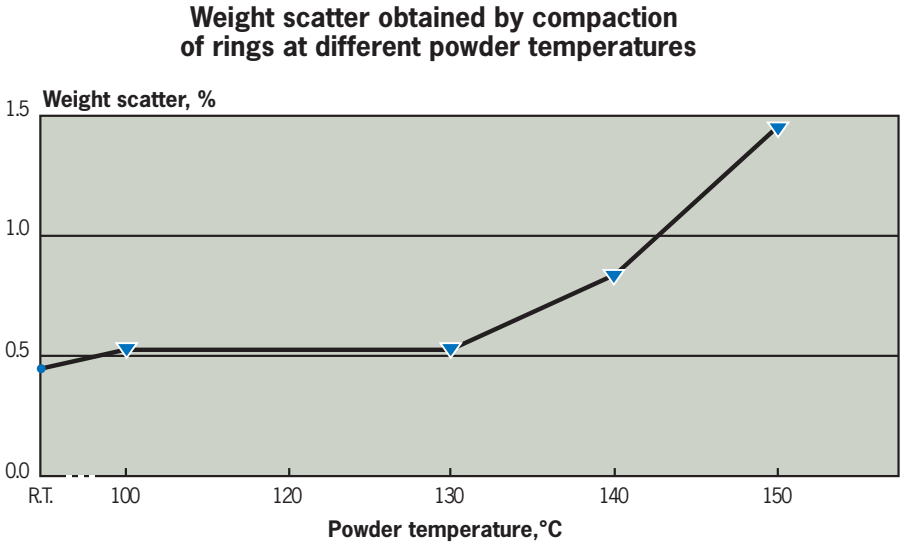


*Figure 8. Influence of powder temperature on weight scatter in %.*

As can be seen the weight scatter is very stable up to 130°C, but increases when the temperature is raised. The effect of temperature on green density for a Densmix™ containing Distaloy AE + 0.3% C is shown in figure 9. Distaloy AE has composition of 1.5% Cu, 0.5% Mo and 4% Ni balanced with Fe.

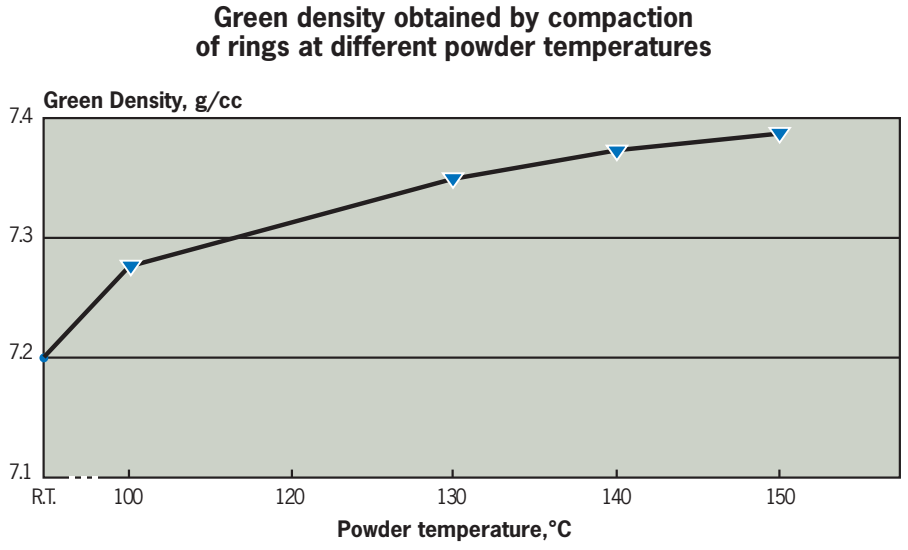


*Figure 9. Influence of powder temperature on green density, die temperature 150°C.*

Green density shows a significant increase between room temperature to 100°C and 130°C but only a slight increase can be seen between 130 to 150°C.

On the other hand green strength is continously increased more significantly by increased temperature, which is shown in figure 10.

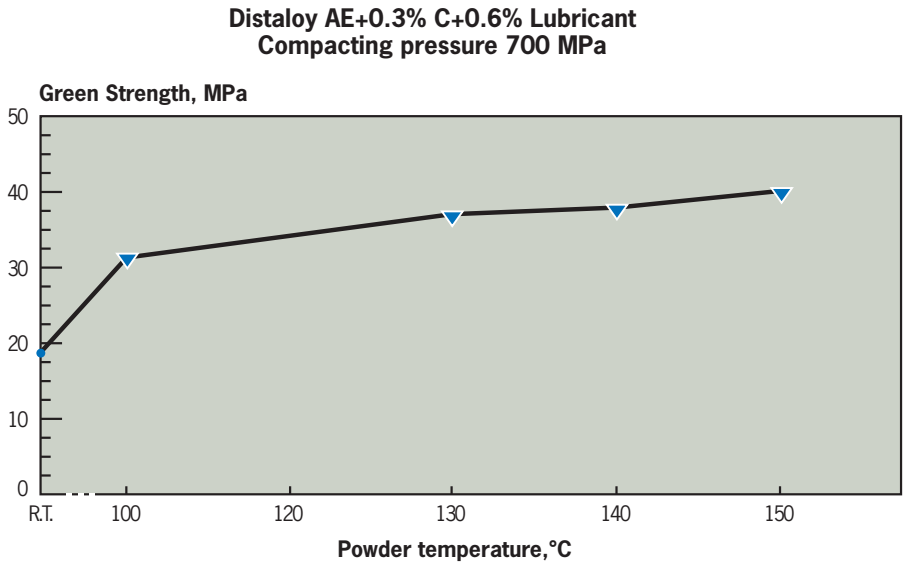


*Figure 10. Influence of powder temperature on green strength, die (tool) temperature 150°C.*

If the powder is kept in a heater for a long time or is reheated several times it does not affect the powder properties in a significant way. Tables 1 and 2 show the effect of heating time and cyclical heating and reheating upon Flow, AD and GD.

**Table 1.** Influence of storing time at 130°C on some powder properties for a Densmix™ containing Distaloy AE + 0.6% Graphite**.**

| Storage time* (h) | Flow* (s/50g) | Apparent density* (s/50g) | Green density** ($g/cm^3$) |
|---|---|---|---|
| 0.1 | 26.5 | 3.15 | 7.29 |
| 2.0 | 26.2 | 3.15 | 7.30 |
| 8.0 | 26.3 | 3.14 | 7.29 |
| * At 130°C, ** At 600 MPa | | | |

**Table 2.** Influence of the number of heating cycles on some powder properties for a Densmix™ containing Distaloy AE + 0.6% Graphite**.**

| Number of heating cycles to 130°C | Flow* (s/50g) | Apparent density* (s/50g) | Green density** ($g/cm^3$) |
|---|---|---|---|
| 1 | 26.5 | 3.15 | 7.29 |
| 2 | 26.4 | 3.13 | 7.30 |
| 3 | 26.2 | 3.15 | 7.29 |
| 4 | 26.5 | 3.14 | 7.29 |
| * At 130°C, ** At 600 MPa | | | |

## 4.1 Demands on Temperature Control

As can be seen in the above diagrams the temperature used in warm compaction affects all properties, more or less, and what absolute working temperature one chooses allows optimisation of different desired properties. The powder technology sets the ground conditions for the level of working temperature. See figure 11. It shows the set of powder/tool-temperatures that can be used with the Densmix™concept.

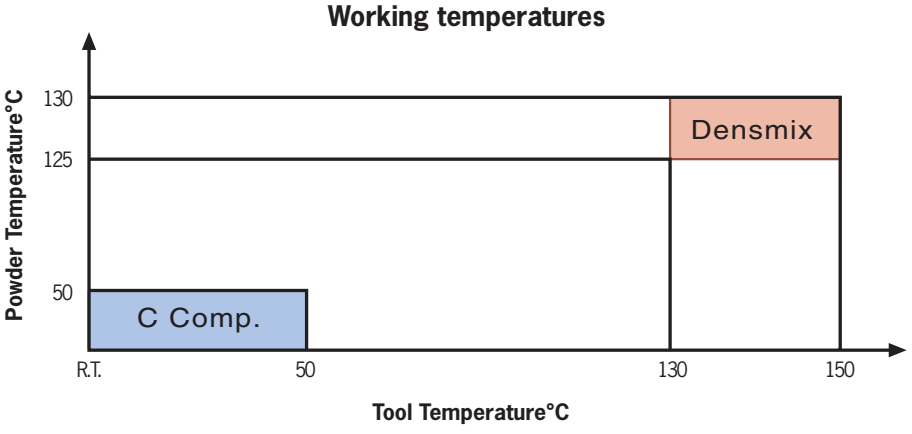


*Figure 11. Working temperatures of Densmix™. (C Comp. = Cold/conventional Compaction).*

It is important to note that the temperature range represents the *temperature level*. The *temperature variations* around a chosen level are critical to the consistency of the products produced by the warm compaction process. For the Densmix™concept a scatter of maximum ± 2.5°C is recommended within the whole system.

# 5 Powder heaters

The choice of heating method for warm compaction applications depends on two factors: temperature and time – the required temperature and temperature distribution of the items to be heated, and the time allowable for equipment pre-heating if productivity goals are to be met.

The powder must be heated uniformly, and care must be taken to avoid excessive temperature variation – especially localised peak temperatures (temperatures above the powder's working range). Bear in mind that powder has a relatively low thermal conductivity.

The ideal solution would be to heat each powder particle simultaneously, either via a large-surface plate heater heating a single layer of powder particles, or using a fluid at the right temperature (gas or liquid) which envelopes all powder particles.

To date, there are three different heating systems developed: Slot Heater, EL-Temp and Abbot. The first two utilize plate heating systems, whereas Abbot is based on the fluid principle.

The Slot Heater's plate heat exchanger warms gravity-fed, free-flowing powder, whereas EL-Temp uses a heated screw feeder (auger). What differentiates the two methods is the shear stress which the powder is exposed to when fed to the filling shoe and tooling. Negligible on the Slot Heater, it is clearly large on the EL-Temp.

The third method, represented by Abbot's heating system, utilizes a more sophisticated principle – fluidisation. By forcing a fluid (in this case, air) through the powder bed, a fluid state is created.

Powder heating is the most time consuming of all the component heating procedures in the warm compaction process for the Slot Heater (see Chapters 6 and 7 for further details). As mentioned above, this is because of the powder's low thermal conductivity and its sensitivity to peak temperatures.

A detailed description of the Slot Heater method follows.

## 5.1 Slot Heater

The Slot Heater operates as a heat exchanger where oil is used as heating media and has a capacity - at standard measures - of approximately 4.5 kg/minutes at 130° C. See figure 12 on page 24. If the produced parts are 450 g each, this permits a production rate of ≈10 parts/minute.
Depending on the apparent density of the powder mix the mass in the heat exchanger is approximately 25-30 kg.

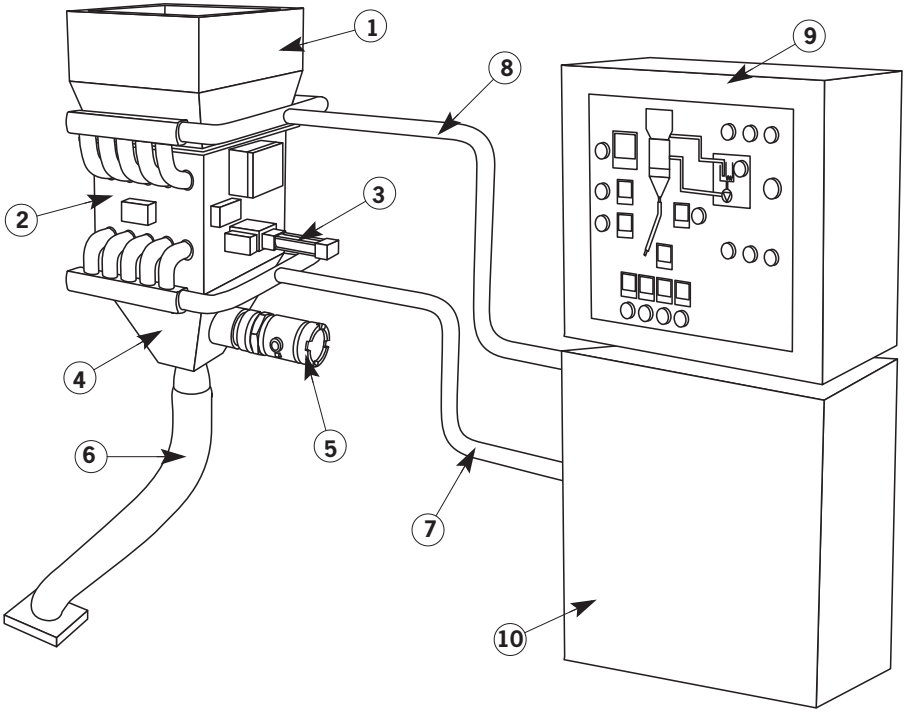


1. Hopper
2. Heat exchanger
3. Pneumatic valve
4. Cone
5. Level sensor
6. Hose
7. Oil inlet
8. Oil return
9. Control cabinet
10. Oil (pump) heater

*Figure 12. The Slot Heater unit.*

**Heating system**

The Slot Heater is equipped with heating systems at three positions: the heat exchanger, the cone and the hose. Powder in the heat exchanger fills between the slots which are heated by circulating oil, pre-heated in an oil heater. The heating time of the powder from start-up at room temperature to operating temperature (130° C) is 1-1.5 hours. Only oil specifically intended for heating purposes may be used.

After the heat exchanger is the cone which is heated by foil elements positioned by glueing, outside the four walls. This is done in order to maintain the powder temperature, not for heating up the powder.

After the cone a transport hose maintains the powder temperature by a resistance wire twisted around the hose, before the material enters the stationary feeder on the filling shoe.

### Pneumatic system

In order to keep an accurate temperature within the powder, it is important that the emptying of powder from the heat exchanger down to the cone, takes place from all the slots simultaneously. This emptying is controlled by an inductive level sensor built-in to the cone and then connected to the pneumatic valve. Required air pressure for the valve is 5-6 Bars. The level sensor makes it possible to always have a constant powder level from the cone down to the filling shoe.

### Oil heater

The system for heating oil consists of a heat exchanger, oil pump, open oil tank, expansion chamber, level sensor, thermocouples and high temperature sensor, and resistor elements. The oil is heated in the open tank by the resistor elements and pumped through the heat exchanger. Since this is an open system, the oil pressure must always be kept below two Bar.

### Control Cabinet

In addition to the control equipment for the Slot Heater the control cabinet includes control equipment for the tooling such as filling shoe, die, upper punch and adaptor table. Note: As a standard the maximum power effects on each of the units above is 3.5 kW.

### Insulation

In order to avoid heat losses the Slot Heater system (the heat exchanger, the cone and the hose) is totally insulated outside with dense silicone cell rubber. The insulation material has to be glued on the actual surfaces by using heat resistant silicone glue.

### Installation

The Slot Heater can be mounted directly on the press using a support. See figure 13. Or it can be mounted on a mobile support.

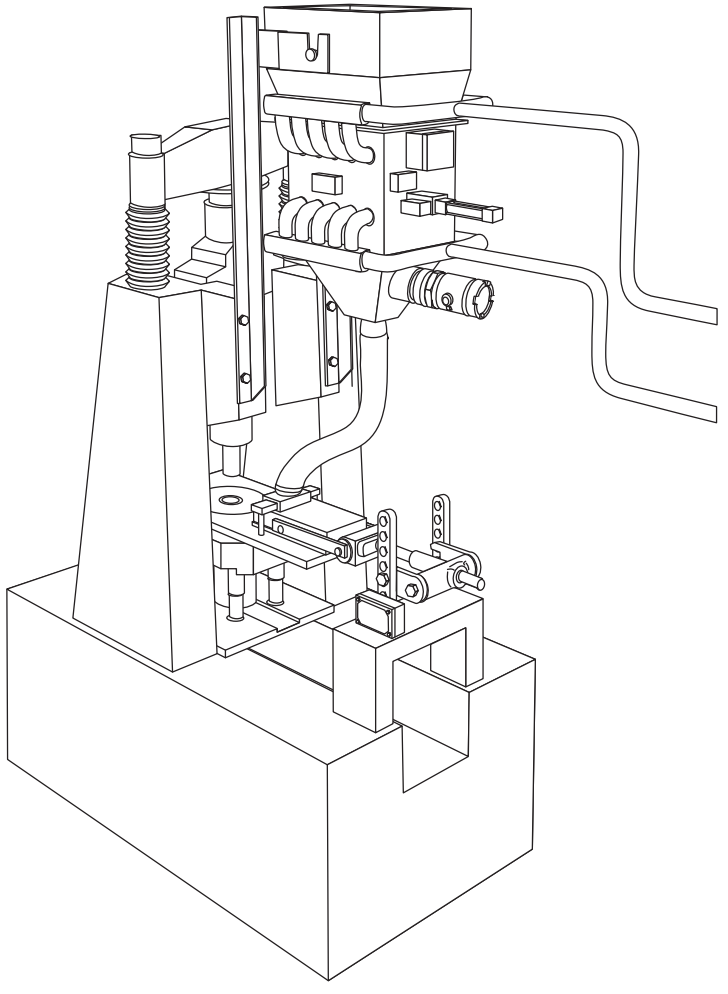

*Figure 13. Slot Heater mounted on a press.*

To avoid interruption of powder flow, due to air pockets or zones of "dead" powder in the hose, it should be mounted at an angle as steep as possible. The hose should be in line with, and as close as possible to perpendicular to the stationary feeder. Figure 14 illustrates the moving filling shoe in feeding position.

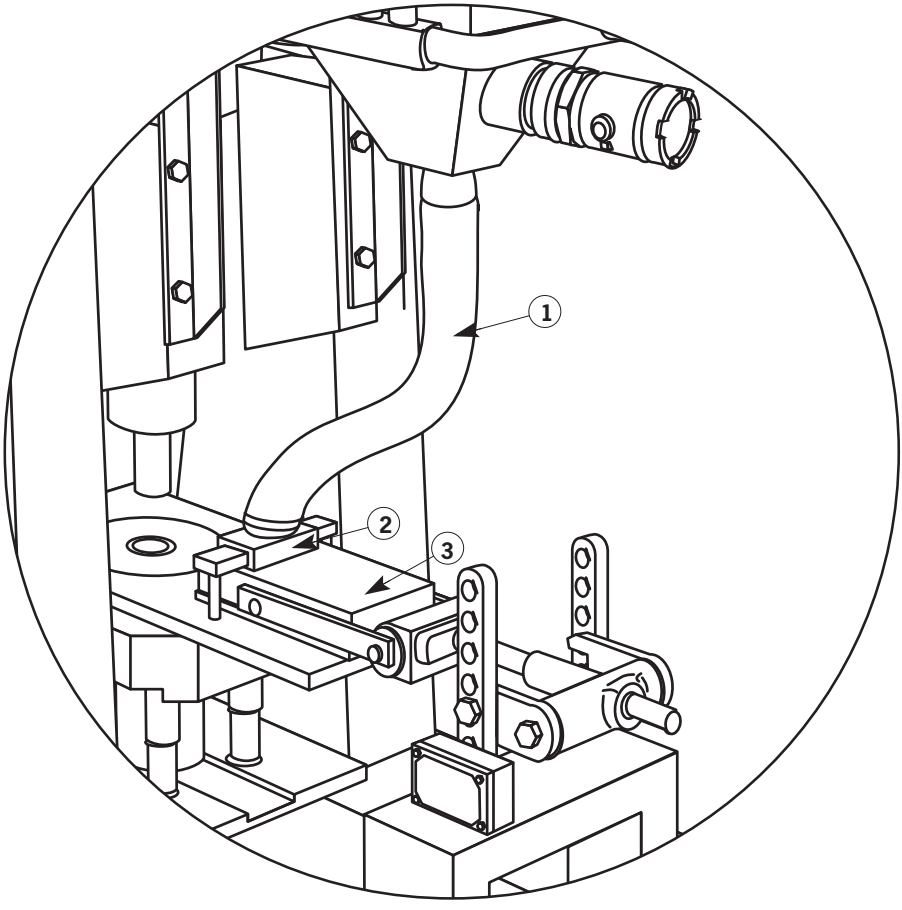


1. Feeding hose
2. Stationary feeder
3. Moving filling shoe

*Figure 14. Illustration of feeding hose, stationary feeder and moving filling shoe (in feeding position).*

An angle in the feeding hose of not less than 65° is recommended. Thus the length of the hose must be just right. This is shown in figure 15 with an example having a hose length of 0.7 m. The hose moves vertically during the compaction cycle and so must be just long enough to allow free movement without causing distortion of the angle and poor powder flow.

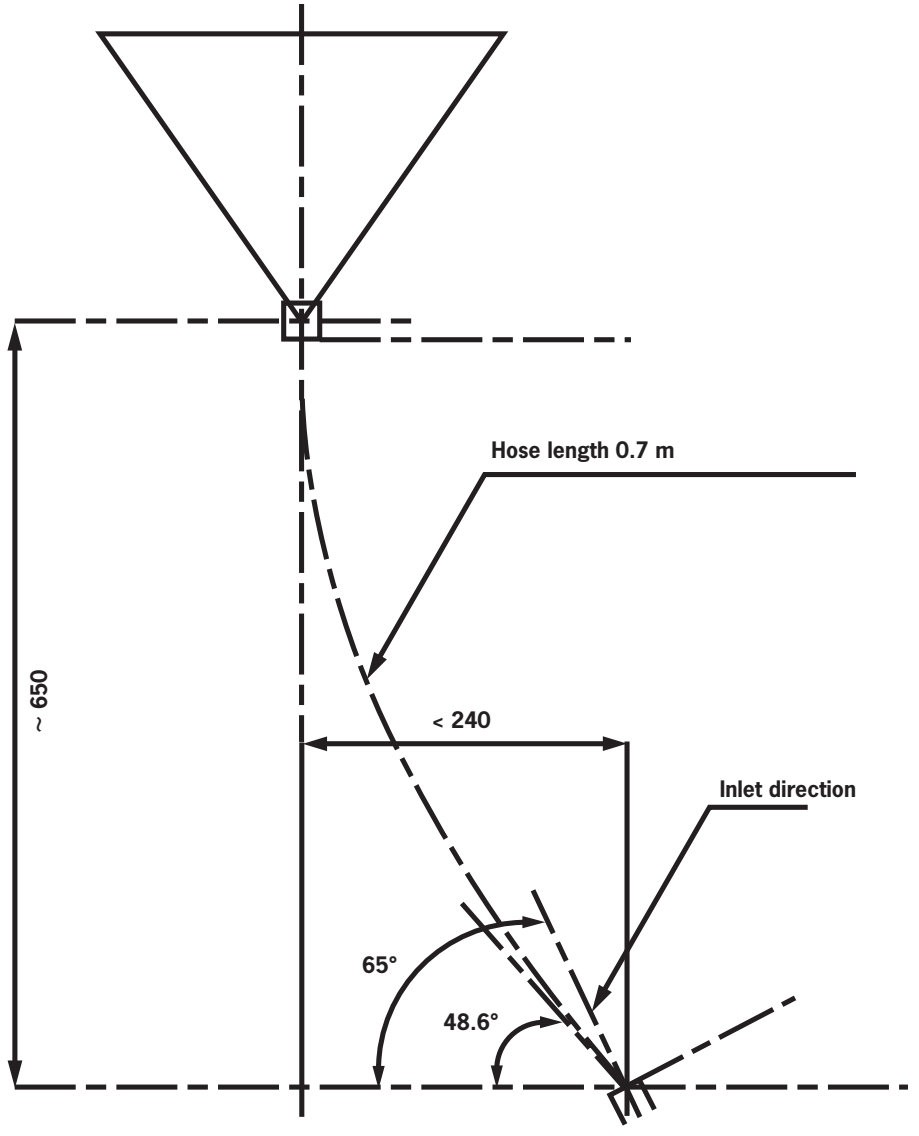


*Figure 15. Maximum hose bending / 0.7 m hose.*

# 6 Filling Shoe

This section presents the special filling shoe system recommended for Slot Heaters but also more general aspects on filling shoes for warm compaction. Since the temperature affects the powder properties (see Chapter 4) it is of great importance to maintain the proper powder temperature within the filling shoe, accomplished by proper *heating* and *insulating*.

The filling shoe concept for Slot Heaters consists of a stationary feeder and a moving filling shoe. See figure 16. The reason for this is the sensitivity of the hose, which only permits the Slot Heater to move slightly in the horizontal direction.

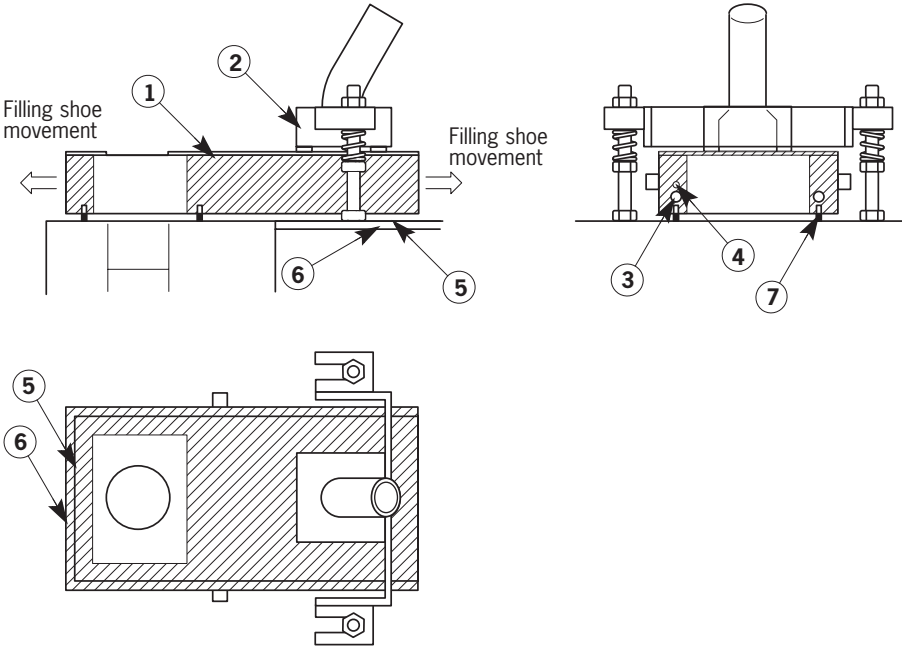


1. Moving filling shoe
2. Stationary feeder
3. Cartridge heater
4. Thermocouple, (optional)
5. Foil element, (optional)
6. Insulation
7. Sealing strip

*Figure 16. Filling shoe design for warm compaction.*

**The filling/pressing cycle**

The parts essential to the filling/pressing cycle are shown in figure 16. A stationary feeder and a moving filling shoe feed powder down into the die cavity. The amount of powder in the moving filling shoe is normally equal to that required for three or four pressed components, to ensure good filling of the die cavity. The full cycle is as follows:

1. Powder moves down from the moving filling shoe into the die cavity.
2. The moving filling shoe moves back to its end position.
3. The powder is compacted in the die; at the same time, the moving filling shoe is filled with new powder from stationary feeder.
4. The pressed part is ejected from the die; the moving filling shoe moves forward and acting as sliding valve, closes off the flow of powder from the stationary feeder.
5. The compacted part is removed, often by a robot arm, or by the action of the moving filling shoe, which then returns into position under the stationary feeder to begin the filling cycle again

## 6.1 Heating system

As described at the start of Chapter 5, a smooth and thermally controlled heat transfer to the powder is necessary. At the filling shoe, the powder's temperature is then best maintained by using cartridge heaters. Placed symmetrically in the shoe's side walls, they provide a fairly even temperature distribution, and ensure that an appropriate temperature equilibrium is maintained as the powder is transferred to the die's cavity.

In order to heat the moving filling shoe, cartridge heaters are normally used, but in some cases also foil elements. See figure 16 on page 29.

It is important to protect the powder from direct contact with the heat source and make sure that the heat is transported to the powder in a uniform way. If the heaters are put inside the filling shoe walls, the heat is more uniformly spread and the system not so sensitive to overheating.

The temperature control is also critical to prevent overheating; if cartridges are used, it is wise to also use built-in thermocouples (at least one). Recommended tolerances for hole diameters of the cartridge heaters are according to ISO F8.

If foil elements are used, the proper way to position them is by glueing (silicon glue) outside the filling shoe.

If no built-in thermocouples are used in the cartridge heaters it is important that a thermocouple is located inside the wall, close to one of the cartridge heaters (~13-15 mm centre to centre) and to a depth of approximately half of the length of the cartridge heater. In the case of foil elements, the most suitable thermocouple is in the shape of a thin plate located between the foil element and one of the walls of the filling shoe.

(Thermocouples of type “J” are standard on a Slot Heater). The stationary feeder is connected to the hose and if the stationary feeder is fairly large, additional heating might be necessary.

## 6.2 Insulation

In order to maintain a uniform temperature without too high heat losses, insulation of the filling shoe is needed; a basic truth for the whole warm compaction concept. The better protection between hot and cold, the better the temperature control (not so large temperature gradients) and economy. Thus the filling shoe should be insulated, where place, space and functionality permits.

The most commonly used insulating material is dense silicon cell rubber applied on the surfaces by heat resistant silicon glue.

# 7 Tooling

Elevated temperatures, even at moderate increases as in warm compaction, require adequate heating and cooling devices on the tooling. This is in order to have the proper temperature for pressing in the die and to protect the press from higher temperatures.

The tooling set is normally heated at three different locations; *die, adaptor table* and the *upper punch*.
Number, location and energy output of the heaters is dependent on material, geometry and surrounding heat flow characteristics such as ambient temperature and air flow, but also on the cooling configuration (water, oil, gills/flanges etc.).
This section gives some guidelines in order to understand, design and maintain proper pressing conditions in respect to tooling for warm compaction.

## 7.1 Power needed for heating and maintaining the proper temperature

In order to have enough power to heat the tooling one must first consider in what time the tooling has to be heated up from room temperature and secondly, the heat that has to be put into the tooling during operation at the proper temperature (steady state). Thus two separate calculations have to be made in order to know which phase is dimensioning the power need of the tooling.

### Heating from room temperature to operation temperature

A widely used approximate calculation method, when predicting the power need for heating a tool, is based on the heat capacity, heating time and the mass of the tool, assuming that the heat losses are zero. This basically wrong assumption (according to figure 19 on page 35 and figure 20 on page 36 ) is corrected by assumptions about the heat losses or the use of safety factors. Different safety factors are used by different authors in the literature. In this case a conservative figure has been chosen, SF=2.
See equation 7.1.

$$P = \frac{m \cdot C_P \cdot \Delta T}{t} \cdot SF \qquad \text{(eq. 7.1)}$$

m = heated mass in kg
$C_P$ = average heat capacity over the temperature range in J/kg · K
$\Delta T$ = temperature range in K
t = heating time in seconds
P = Power need – effect in W (J/s)
SF = Safety Factor

Heating can be compared to a lab beaker which is to be filled to a certain level during a given time period. The flow to the beaker (or system, as it is called in the study of Thermodynamics) is the controlling parameter. Flow F = volume per time unit. Flow can be equated with the energy/time unit required to heat the tool, volume is the amount of thermal energy supplied to the system ($mC_p\Delta T$), and time is the targeted heating interval. The figure below describes a closed system with no losses. See figure 17.

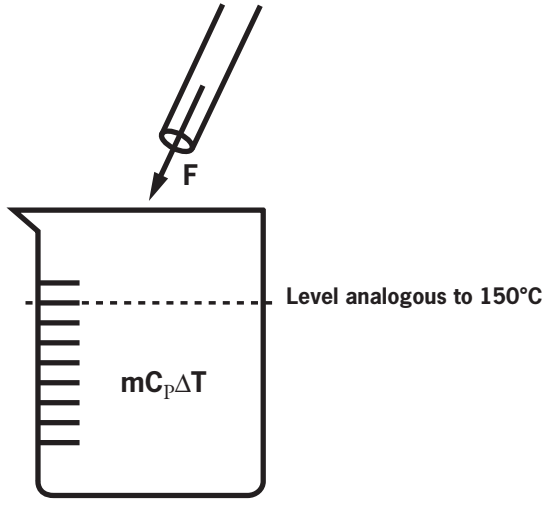


*Figure 17. A lab beaker which is to be filled to a certain level during a given time period.*

In reality, however, heat losses do occur, and they are proportional to the temperature level to be attained in the material heated. Losses increase with increasing temperature, presupposing that room temperatures remain constant. Losses during heating are likely to be smaller than at equilibrium. Our beaker example thereby includes 'holes' whose size increase with increasing temperature. See figure 18 on page 34.

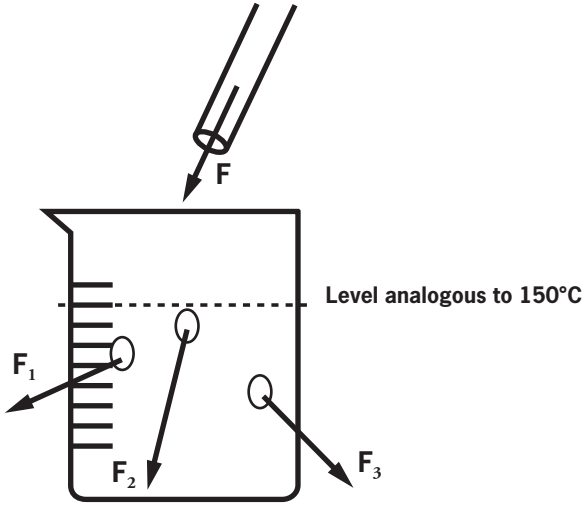


*Figure 18. Losses in the system.*

**Maintaining the proper temperature at steady state**

During heating (as opposed to equilibrium), the thermal inflow is greater than the sum of heat losses, as a given level must accumulate in the tool.
At equilibrium, our 'beaker' is 'full' but, to remain so, a continuous heat flow must be supplied which fulfils the following criteria:

$$F=F_1+F_2+F_3$$

The thermal equilibrium that has to be maintained in the tooling is constituted by different heat sources and heat “consumers” or losses. In order to have a thermal equilibrium, at the proper temperature, a certain amount of heat energy has to be stored, or maintained, within the die, adaptor table and upper punch. This energy depends on the mass and heat capacity of the tooling. See figure 19 on page 35.

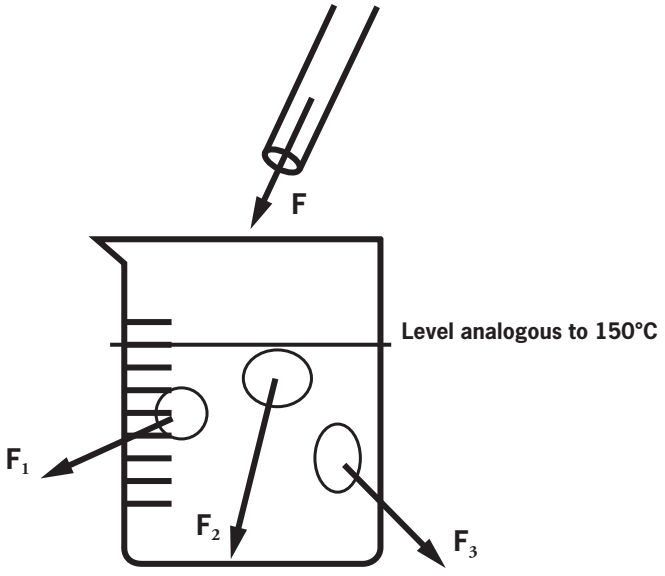


*Figure 19. Retaining heat. At equilibrium (steady state), inflow must match outflow.*

The three 'holes' in our beaker symbolize the three heat loss sources:

- Radiation.
- Conduction.
- Convection.

The heat losses in the tooling are schematically shown. See figure 20.

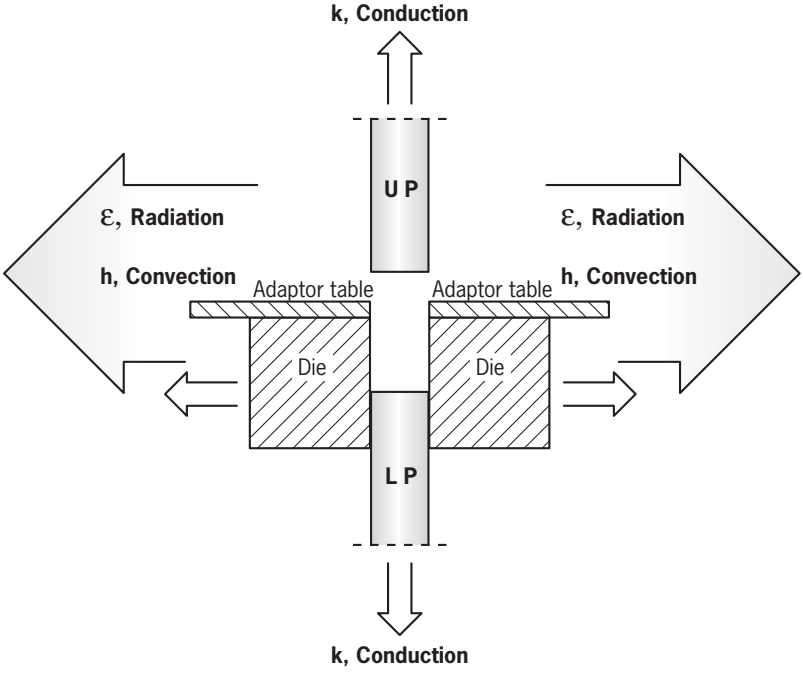


*Figure 20. Thermal losses for the die set in a press.*

As can be seen three different types of heat losses, via heat transports, exist. These different losses can be expressed according to equations 7.2-7.4 in the case of stationary conditions:

**Conduction:**

$$P_{Condu} = A \frac{k}{\Delta x} \Delta T \qquad \text{(eq. 7.2)}$$

**Radiation:**

$$P_{Rad} = A \varepsilon \sigma (T_1^4 - T_2^4) \qquad \text{(eq. 7.3)}$$

**Convection:**

$$P_{Conv} = A h (T_1 - T_2) \qquad \text{(eq. 7.4)}$$

In these equations: where $P$ is the energy loss per time unit (W), $A$ is the exposed area, $k$ the thermal conductivity of the material, $T$ the temperature, $x$ the heat transport distance in the solid media, $\varepsilon$ the thermal emissivity of the radiating surface, $\sigma$ the Stefan-Boltzmann constant and h the heat transfer coefficient between gas bulk and material surface.

By these equations it is for instance understood that the surface of the boundary where the heat transfer is taking place, in this case the tool surfaces, plays an important role. A more compact tooling, with a low ratio of surface to volume, gives lower losses.

In reality the tooling is put together by different materials with different geometries. This will lead to a very complex situation when determining the total heat transfer coefficient of the system, which in turn gives difficulties when predicting the power needed to heat and maintain the tooling at a proper temperature. This can only be done in a reasonable time with the help of a FEM-program for instance, if precise calculations have to be made.

A cheaper and simpler way is to estimate the heat losses in different toolings from practical experiences, in order to know the power needed. See the three examples in the next section of this chapter.

By the equations 7.2-7.4 it is also understood that every temperature gradient (variation in temperature) will give a heat flow from the warmer to the colder regions. Thus it is of importance to have uniform, symmetrical heating in the die.

Even if the different parts in the tooling are heated symmetrically, there will be temperature gradients in the tool. A 3-D sketch from a computer simulation (FEM) made at IFAM in Bremen [23] shows how the temperature gradient could appear in a cylindrical tool. See figure 21 on page 38.

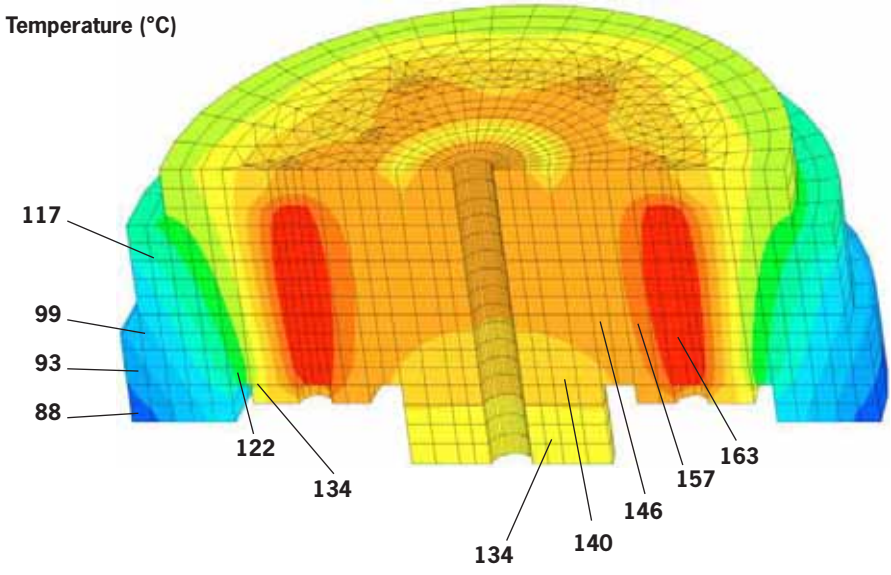


*Figure 21. Temperature distribution in a cylindrical die calculated with FEM (published with the permission of IFAM, Bremen [23]).*

This simulation shows that it is of greatest importance to trim the system by checking the cavity surface and the upper punch temperature before pressing, at stable temperature conditions.

## 7.2 Examples of Warm Compaction Applications

In this section three examples are given to describe a range of applications using warm compaction tools. The first example is a relatively small ring tool with a readily heated small die. The second example is a laboratory tool used to produce fatigue test bars; and the third is a rather large tool which requires heating of a large mass.

The calculations given in these examples show how it is possible to work out the power need for a particular tool: to fairly easily calculate heat losses and the effect of installed heat cartridges. All three examples describe a situation where a tool is heated from room temperature (20°C) and a stable operating tool temperature of 150°C is maintained.

**Example 1. Ring tool (die)**
A ring tool is used in an automatic, mechanical 45 ton, Dorst press at Höganäs AB adjusted for warm compaction. The die in this tool is presented in figure 22 below.

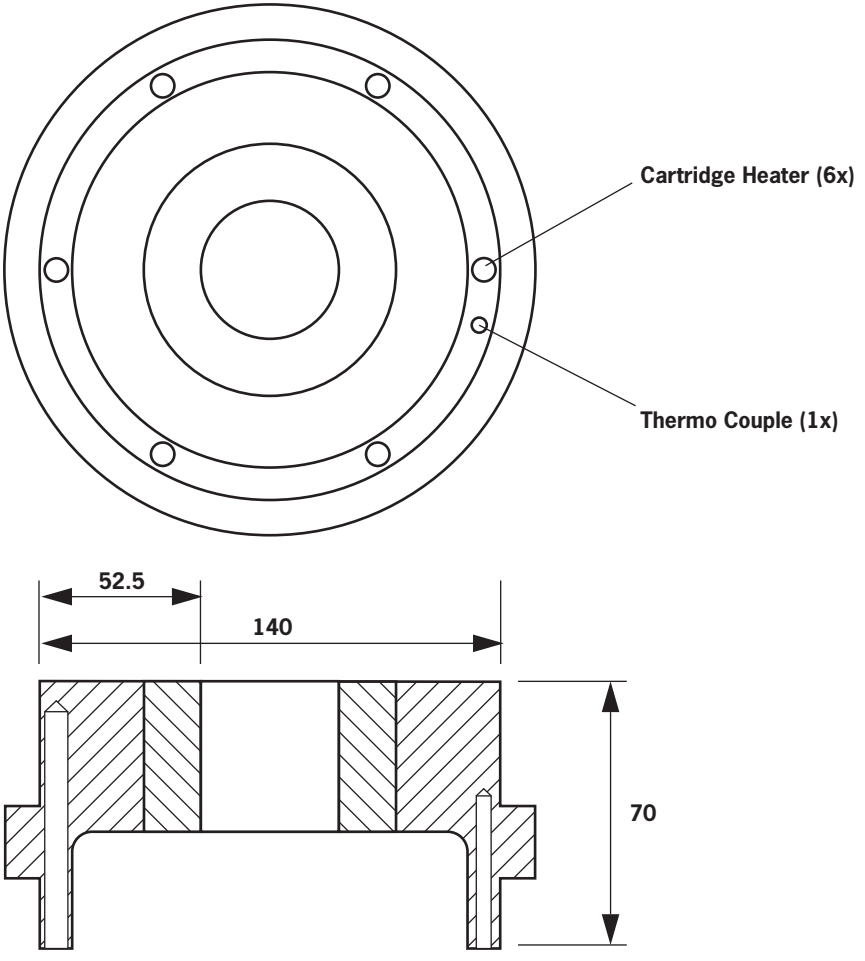


*Figure 22. Ring tool at Höganäs AB.*

Six cartridges with an effect of 250 W each are used to heat the die. This corresponds to a power need (for the die) of 1.5 kW.

### Heating the die

By using equation 7.1 and chosing a wanted minimum heating time of the tool it is simple to calculate the power need. How do we select the heating time? One limitation is the powder heating time which normally is about 1 hour depending on what kind of heater is used. Another is how fast a thermal steady state can be obtained, which is a function of the temperature, tool mass, geometry and temperature control mode. The die dimensions are approximated to 140 mm diameter and 70 mm height.

$m = \rho \cdot V$, calculated by volume and density. (eq. 7.1)

$\rho$ = 7800 kg/m$^3$, steel

V = 0.00108 m$^3$

$m$ = 8.4 kg

$C_P$ = 460 J/kg·K, steel

$\Delta T$ = (150-20) = 130 K

t = 1 hour = 3600 s

P = W (J/s)

SF = 2

$$V = \frac{0.140^2 \cdot \pi}{4} \cdot 0.70 \text{ m}^3 = 0.00108 \text{ m}^3$$

$$P = \frac{8.4 \cdot 460 \cdot 130}{3600} \cdot 2 = \underline{0.28 \text{ kW}}$$

As can be seen, calculations without any knowledge about the losses, will lead to totally wrong conclusions about the power need.

### To maintain the temperature at steady state

Die losses are estimated according to equations 7.2-7.4 and with the help of additional equations in reference [18]. The different boundaries/areas where heat transport takes place are described in the next figure. See figure 23 on page 42.

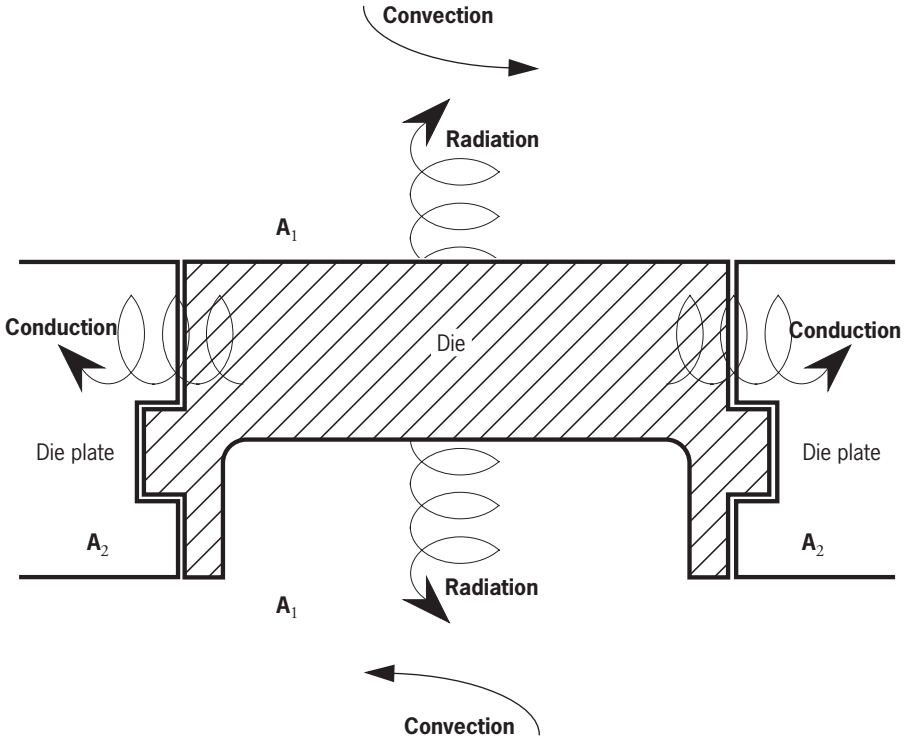


*Figure 23. Heat transport boundaries in a ring tool.*

1. Radiation losses:

   The emissivity was taken as for oxidised steel (=0.8) and the projected area ($A_1$ in figure 23 on page 42 ) calculated to 0.01539 $m^2$ (with the cavity). Radiation from the die to the surroundings and radiation from the die to the tool set was calculated assuming that the tool set was a plate parallel to the surface of the die.

   **Total radiation losses: 63W**

This means that radiation losses are approximately 2 $kW/m^2$ for a die with 150°C and surrounding temperature of 20°C.

2. Conduction losses:

   The die is fitted into the die plate, but there is still a small air gap between the die and the die plate ($A_2$ in figure 23 on page 42 ). The conduction losses can be calculated with the assumption that the temperature on the surface ($A_2$) on the tool is in the range of 100°C, neglecting the heat source and calculating the only known surface - the die cavity - as 150°C. Approximate heat conductivity is 45 W/mK (steel) and transport distance of 0.0615 m = cavity surface - die surface = Δx, in (eq. 7.2).

$$P_{Condu} = \left\{ A \cdot \frac{k}{\Delta x} \Delta T \right\} = 0.140 \cdot \pi \cdot 0.070 \cdot \frac{45}{0.0525} \cdot (150 - 100)\ W = 1319\ W = 1.3\ kW$$

   **Total conduction losses: 1.3 kW**

3. Convective losses:

   The only surfaces exposed to convection are the horizontal surfaces A1. If no forced convection is exerted on the tool (i.e. no "wind" or pressure air) the losses because of natural convection can be calculated according to convection on a circular plate from the top and the bottom assuming the surface temperature at 150°C and the surrounding gas bulk temperature at 20°C. For the top this gives 13 W or 1 kW/m$^2$ and for the bottom 6 W or 0.5kW/m$^2$ for this cylindrical tool.

   **Total convective losses: 13 W (top) and 6 W (bottom)**

Total losses for the ring tool can thus be expressed as the sum of the different losses:
63 + 1319 + 13 + 6 ≈ **1.4 kW**

***Conclusion:***
As the power need for the heat losses are higher than the need for heating the die, the losses are dimensioning for the system and the power need should be approximately 1.4 kW. The chosen cartridges have a power need of 1.5 kW which means that it is often better to estimate the heat losses than to calculate the power need from the heat capacity. It is also interesting to note that the convective and radiative losses seem to be very small and conduction is the dominating heat loss.

**Example 2. Fatigue testing bar tool**

A tool for pressing fatigue testing bars at Höganäs AB. See figure 24. The outer diameter of the die is 340 mm and the height 50 mm.

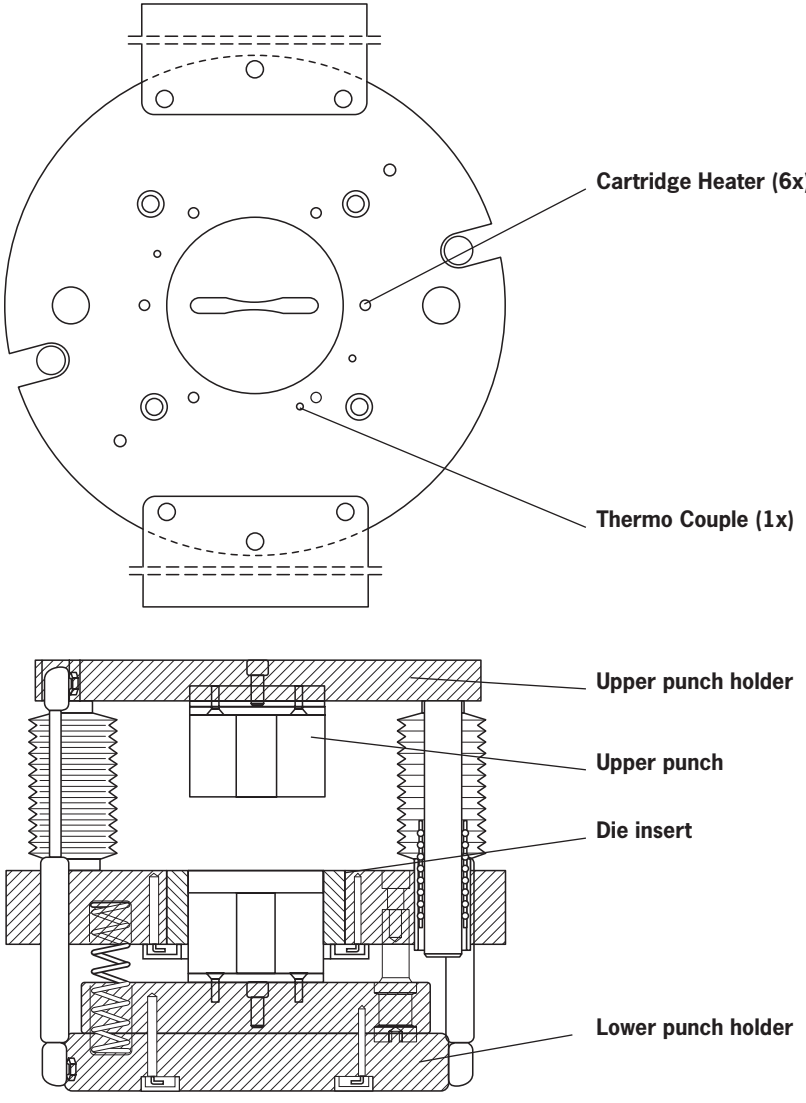


*Figure 24. Fatigue bar pressing tool at Höganäs AB.*

In this case heating is accomplished in four different locations:
1. Die, 2. Lower punch holder/bottom plate, 3. Upper punch and, 4. The upper punch holder.

The die assembly as presented in figure 24, is placed directly in a hydraulic press, where the pressing force comes from a hydraulic cylinder above. The power need for this tool is understood by the number and capacity of the different heating elements.

1 : 6 cartridge heaters with 200 W ⇒ 1200 W
2 : 6 cartridge heaters with 250 W ⇒ 1500 W
3 : 2 band elements with 250 W ⇒ 500 W
4 : 3 cartridge heaters with 300 W ⇒ 900 W

**Total amount of power: 1200W + 1500W + 500W + 900W = 4100W = 4.1 kW**

This means that the power supply should, at a minimum, be able to provide the tooling with 4.1 kW. The different heated locations 1-4 are controlled and fed separately with electricity.

How was the power needed estimated before the tool was adjusted for warm compaction? As mentioned before two calculations have to be made; one for the heating from room temperature to the operation temperature (*Heating the die*), and one for the operation temperature (*To maintain the temperature at steady state*). In the calculations below only the die has been calculated.

### Heating the die

The time chosen for heating the die is 1 hour and die dimension is a cylindrical plate of 350 mm diameter and 50 mm height.

$m$ = $\rho \cdot V$, calculated by volume and density.
$\rho$ = 7800 kg/m$^3$, steel
$V$ = 0.00481 m$^3$
$m$ = 37.5 kg
$C_P$ = 460 J/kg·K, steel
$\Delta T$ = (150-20) = 130 K
$t$ = 1 hour = 3600 s
$P$ = W (J/s)
SF = 2

$$V = \frac{0.350^2 \cdot \pi}{4} \cdot 0.05\ m^3 = 0.0048\ m^3$$

$$P = \frac{37.5 \cdot 460 \cdot 130}{3600} \cdot 2 = \underline{1.25\ kW}$$

In this case the calculated power need is somewhat higher than the actual effect of the cartridges in the die (1200 W). In reality this tool reaches steady state temperature after approximately 40 minutes.

**To maintain the temperature at steady state**

Assuming that the die is a platelike cylinder with the dimensions given above, hanging freely in the air (negligible conduction), this obviously means that the conduction losses also are negligible. In this case only the radiation and convective losses are calculated. The following calculation can be made:

1. Radiation losses.

   With an external surface, calculated as follows:

$$A = \frac{0.340^2 \cdot \pi}{4} \cdot 2 + 0.340 \cdot \pi \cdot 0.050 \ \ m^2 = 0.235\, m^2$$

   (and the heat losses calculated at approximately 2 kW/m$^2$, as in Example 1), then the resulting total radiation loss in this case would be:

$$\mathbf{P}_{Rad} = 2 \cdot AkW = 2 \cdot 0.235\ kW = 0.47\ kW$$

2. Convective losses.

   For the sake of simplicity, it is convenient to ignore the vertical sides of the tool, since the diameter/height relationship is 340/50. This means that convective losses are calculated (with the help of the result in Example 1) at 1kW/m$^2$ (top) and 0.5 kW/m$^2$ (bottom) thus the convenctive heat losses are calculated as:

$$P_{Conv} = 1 \cdot A + 0.5 \cdot A = 1.5 \cdot A = 1.5 \cdot \frac{0.340^2 \cdot \pi}{4}\ kW = 0.14\ kW$$

   **And total loss is: 0.47+0.14=<u>0.61 kW</u>**

*Conclusion:*

The heat loss calculation indicates that the assumptions made were not totally accurate. There is a minor convective loss from the sides and also there has to be some influence of conduction as well. The conduction losses are though very hard to estimate in this case since the geometry is quite complex. The heat loss from the sides can be estimated, with the help of reference [18], assuming that the envelope surface is a plate, at approximately 65 W, which corresponds to approximately 1.2 kW/m$^2$ if the surface temperature of the tool is 150°C, and surrounding air is at 20°C.

Total losses are corrected to 0.47+0.14+0.07=0.68 kW. The heat loss from the side was practically neglectable. The calculated value for heating up the tool, 1.25 kW, indicates that the 1.2 kW installed would be too little to heat the die. Practical experience say it is enough. In this case we have a tool set that is special as mentioned before.

The tool set is also heated at the lower punch plate which gives lower losses and this is hard to put into the calculations if not using a more sophisticated method. Another reason for getting a higher value is that the whole die is not actually reaching 150°C because of the position of the cartridge heaters and the big dimensions of the die. The cartridges are positioned more to the center were the heat is needed mostly.

**Example 3. Cam lobe tool (die)**
A cam lobe tool is used in a 400 ton Lauffer press at Höganäs AB's laboratory. See figure 25.

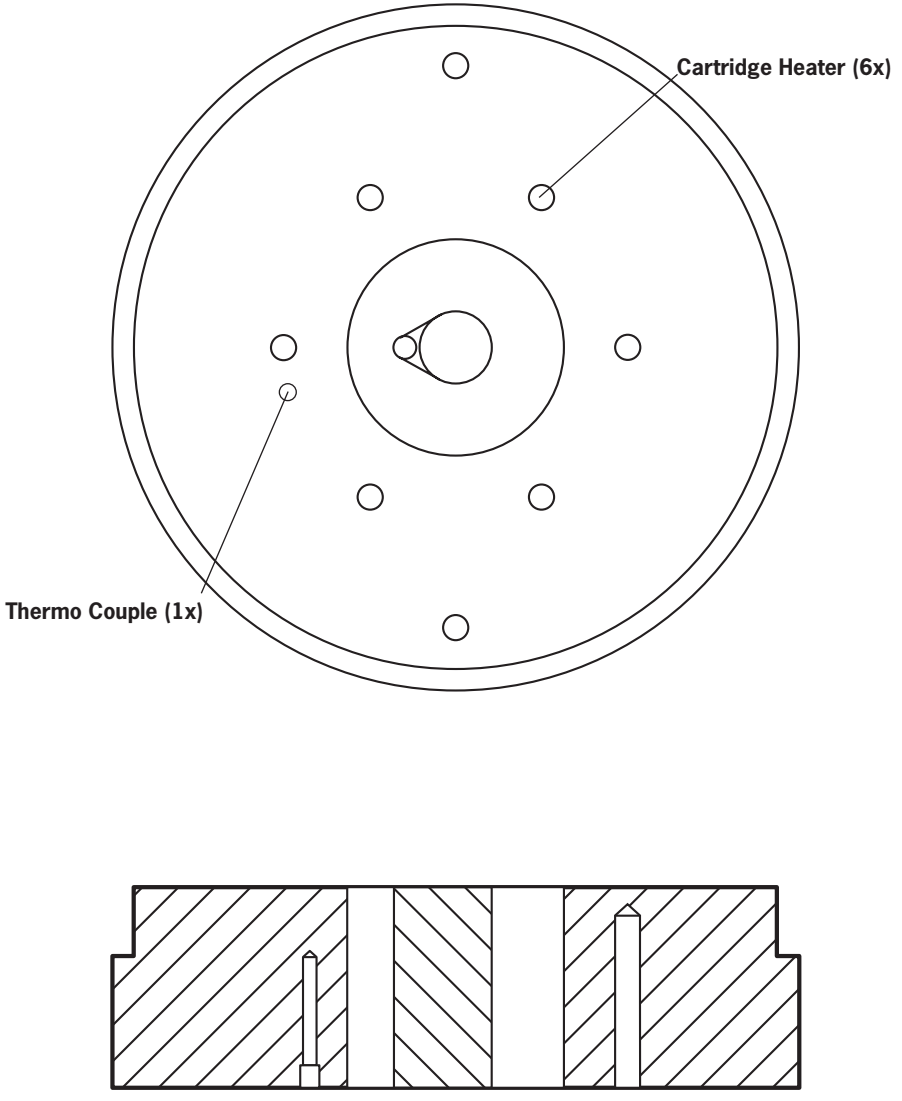


*Figure 25. Cam lobe tool at Höganäs AB.*

Six cartridges with an effect of 250 W each are used to heat the die. This corresponds to a power need (for the die) of **1.5 kW**.

**Heating the die**

The power need for heating up the die is calculated as in Example 1 and 2. Assuming a cylinder of 319 mm diameter and 92 mm height and a heating time of 60 minutes as before.

$$m = \{\rho \cdot V\} = \left\{\rho \cdot \pi \left(\frac{d^2}{4}\right) \cdot h\right\} = 7800 \cdot \pi \cdot \frac{0.319^2}{4} \cdot 0.092 = 57.35 \ \ kg$$

$$P = \left\{\frac{2 \cdot m \cdot C_p \cdot \Delta T}{t}\right\} = \frac{2 \cdot 57.35 \cdot 460 \cdot 130}{3600} = 1.9 \ \ kW$$

The power need for heating the die is **1.9 kW**.

**To maintain the temperature at steady state**

The power need at steady state is calculated as in equation 7.1 with the die fixed in the die plate.

1. Radiation losses.

(2 kW/m$^2$) x (area of upper and lower surfaces):

$$P_{Rad} = \{2 \ \ kW / m^2\} \Rightarrow P_{Rad} = \left\{2 \cdot 2 \cdot \pi \cdot \frac{d^2}{4}\right\} = 2 \cdot 2 \cdot \pi \cdot \frac{0.319^2}{4} = 0.32 \ \ kW$$

2. Convection losses.

(1 kW/m$^2$ for the top) x (top area) + (0.5 kW/m$^2$ for the bottom) x (bottom area):

$$P_{Conv} = \left\{\left(1 \ kW / m^2\right) x \left(\text{top area}\right) + \left(0.5 \ kW / m^2\right) x \left(\text{bottom area}\right)\right\}$$

$$\Rightarrow P_{Conv} = 1 \cdot \pi \frac{d^2}{4} + 0.5 \cdot \pi \frac{d^2}{4} = 1.5 \cdot \pi \frac{d^2}{4} = 1.5 \cdot \pi \cdot \frac{0.319^2}{4} = 0.12 \ \ kW$$

3. Conduction losses.
If transport distance Δx, is approximated as half the diameter, 0.319/2 ≈ 0.150 m, and cavity temperature 150°C and die surface temperature, 100°C:

$$P_{Condu} = \left\{ A \cdot \frac{k}{\Delta x} \cdot \Delta T \right\} = 0.319 \cdot \pi \cdot 0.092 \cdot \frac{45}{0.150} \cdot (150 - 100) = 1.38 \ \ kW$$

$$P_{total} = \{P_{Rad} + P_{Conv} + P_{Condu}\} = 0.32 + 0.12 + 1.38 = 1.82 \ \ kW$$

The power need for steady state is **1.82 kW**

***Conclusion:***
With the two calculation methods in the above example, a higher energy need was predicted than is actually required. This is probably due to larger dies not being heated completely and their temperature gradients being greater than in the case of a smaller tool (for instance, Example 1).

## 7.3 Summary of tool examples and power need calculations

It is clear from the three examples presented, that the calculation methods used here have limitations. When calculating with the actual dimensions of a tool application and the values of cartridges to be installed, it will however, be possible to come up with a reasonably accurate value for the power need in a given situation. You must apply the examples and equations given here with a good understanding of the dimensions and requirements of a particular tool. To make accurate calculations it is vital to use common sense about the heating required for an individual tool.

It should be kept in mind that large plate-like dies tend to distort the models presented here and give higher values than needed. For more accurate calculations, computer models have to be developed and the boundary conditions examined closely.

In order to avoid problems when predicting the power need for heating a tool, both tool heating input and losses must be calculated. Problems will arise with calculations (using equation 7.1) for situations where the heating time is short. With good estimations of the heat losses, calculations of the energy need should be more accurate.

The 'approximate' calculation method used in examples above, is summarized here. This method is valid for maintaining the tool temperature at 150°C.

Where A is the surface area (in $m^2$) at which the heat transport occurs, and x is the distance (in m) from the die cavity to the die surface:

$$P_{condu} = A \cdot \frac{k}{\Delta x} \cdot \Delta T = \frac{A}{\Delta x} \cdot 45 \cdot (150 - 100) = \frac{A}{\Delta x} \cdot 2.250 \text{ kW} \qquad \text{(eq. 7.5)}$$

And where A ($m^2$) is the area of the surfaces in contact with air:

$$P_{Rad} = 2 \cdot A \text{ kW} \qquad \text{(eq. 7.6)}$$

The following values can be derived for convention heat losses:

$$P_{Conv(top)} = 1 \cdot A \text{ kW} \qquad \text{(eq. 7.7)}$$

$$P_{Conv(bottom)} = 0.5 \cdot A \text{ kW} \qquad \text{(eq. 7.8)}$$

$$P_{Conv(vertical)} = 1.2 \cdot A \text{ kW} \qquad \text{(eq. 7.9)}$$

In equation 7.7, A ($m^2$) is top area of the die; in equation 7.8, it is the bottom area, and in eq. 7.9, A ($m^2$) is the surface area.

An important question to be resolved in designing a warm compaction tool is where to place the heat cartridges. They should be placed as close as possible to the die cavity without being so close as to disturb the shrink-fit of the die. In some situations practical limitations will constrain the placement of cartridges.

## 7.4 Clearance and shrink fit

The clearance between punches and die insert and the shrink fit of die inserts in the die should be adjusted at the operation temperature (in the case of Densmix™~150°C), giving the same level of clearance and shrink fit as in a conventional tool for cold compaction. As a matter of fact, all moving parts with close tolerances, exposed to higher temperatures, should be fitted in the warm condition. This is of great importance especially if materials with different thermal expansions are used together in the tool, for instance tungsten carbide and steel. See figure 26 on page 53. Most steels have a coefficient of thermal expansion approximately of 11.5 x $10^{-6}$/K and tungsten carbide ~5.5 x $10^{-6}$/K.

This means that tungsten carbide has approximately half the expansion compared to steel. In this respect a steel tool might be easier to start with, but a more rigid die is always preferred in respect to spring back and residual forces on the component during ejection.

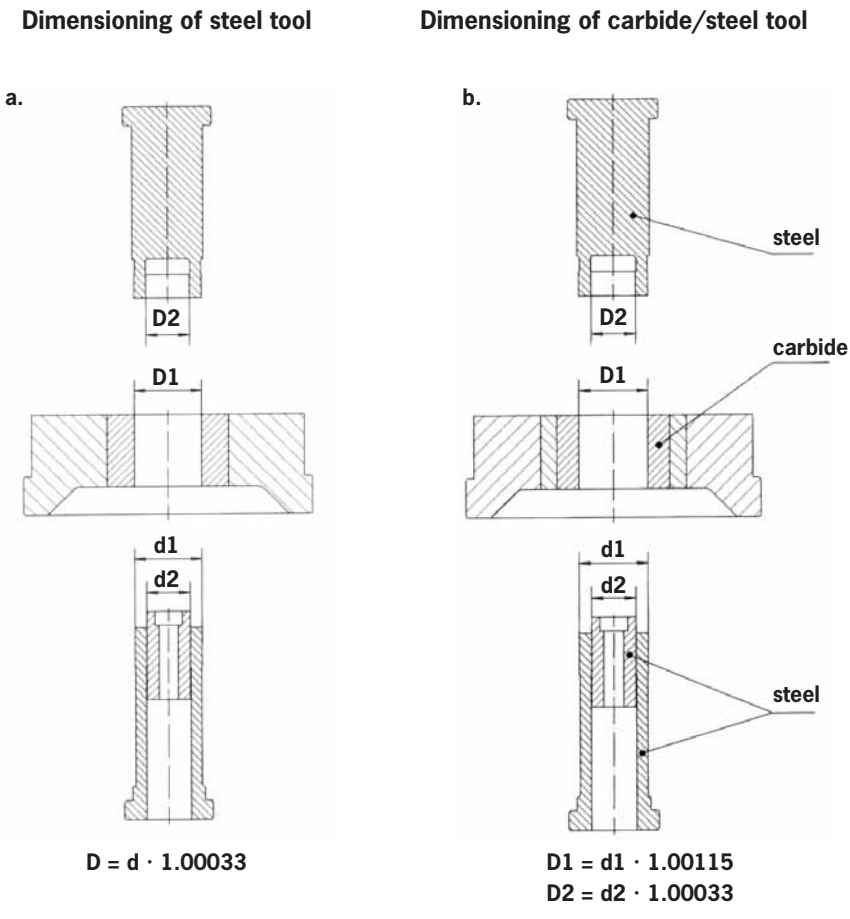


*Figure 26. a. Dimensioning of steel tool. b. Dimensioning of carbide/steel tool. (Published with the permission of Alvier AG).*

## 7.5 Calculation of shrink-fitted dies

The calculations presented here are based on equations and theory from reference [22]. The examples describe the situation for a carbide or a high speed steel insert comparing the "cold" and the warm state.

Let ($d_n$) and ($D_n$) be respectively the inside and the outside, nominal, diameter of the insert and ($d_a$) and ($D_a$) the inside and outside, nominal, diameter of the ring.
Assuming that the inner radial pressure ($P_i$) at compaction end is 200 MPa (N/mm$^2$) it is possible to calculate the diametral relationship I/$\phi$ (I=Interference, $\phi$=common diameter) according to eqation 7.10.

$$\frac{I}{\Phi} = \frac{P_i}{E_n} \cdot \left\{ \frac{1+\alpha^2}{2} \cdot S_1 \cdot \left[ \frac{1+\alpha^2}{1-\alpha^2} - \nu_n + \frac{E_n}{E_a} \cdot \left( \frac{1+\beta^2}{1-\beta^2} + \nu_a \right) \right] - \frac{2 \cdot \alpha^2}{1-\alpha^2} \right\} \qquad \text{(eq. 7.10)}$$

where

$I$ is the interference calculated on the diameter, mm.
$\phi$ is the common diameter, mm.
$P_i$ is the inner radial pressure at compaction end, N/mm$^2$ (assuming 200 N/mm$^2$).
$\alpha$ is the ratio between the inside and the outside diameter of the insert ($\alpha=d_n/D_n$).
$E_n$ is the Young modulus of the material used for the die insert, N/mm$^2$.
$\nu_n$ is the Poisson ratio of the material used for the die insert.
$\beta$ is the ratio between the inside and the outside diameter of the ring ($\beta=d_a/D_a$).
$E_a$ is the Young modulus of the material used for the shrink-fitting ring, N/mm$^2$.
$\nu_a$ is the Poisson ratio of the material used for the shrink-fitted ring.
$S_1$ is a safety factor.

It is also necessary to list all the material properties that are needed. For the coming examples Table 3 is enough.

**Table 3.** Estimated values of significant material properties at 20°C and 150°C.

| Property | Temperature, (°C) | Low alloyed steel | High speed steel (HSS) | ASP 60 (HSS) | Hard metal (10% Co) |
|---|---|---|---|---|---|
| Youngs modulus, MPa | 20 | 206000 | 206000 | 250000 | 580000 |
| | 150 | 196000 | 196000 | 235000 | 555000 |
| Poisson ratio | 20 | 0.296 | 0.296 | 0.296 | 0.22 |
| | 150 | 0.299 | 0.299 | 0.299 | 0.22 |
| Thermal exp. coeff. /°C | 20 | $12 \times 10^{-6}$ | $10.5 \times 10^{-6}$ | $10.5 \times 10^{-6}$ | $5.5 \times 10^{-6}$ |
| | 150 | $12.5 \times 10^{-6}$ | $9.5 \times 10^{-6}$ | $9.5 \times 10^{-6}$ | $5.5 \times 10^{-6}$ |

**Compaction at room temperature (20°C)**

For the insert, let:

$d_n$ = 30 mm

$D_n$ = 50 mm

and for the ring,

$d_a$ = 50 mm

$D_a$ = 125 mm

this means that the ratios $\alpha$ and $\beta$ are:

$\alpha$ = 30/50= 0.6

$\beta$ = 50/125= 0.4

For simplicity it is convenient to calculate the ratios in equation 7.5 above:

$$\frac{1+\alpha^2}{1-\alpha^2} = \frac{1+0.6^2}{1-0.6^2} = 2.125$$

$$\frac{2\cdot\alpha^2}{1-\alpha^2} = \frac{2\cdot0.6^2}{1-0.6^2} = 1.125$$

$$\frac{1+\beta^2}{1-\beta^2} = \frac{1+0.4^2}{1-0.4^2} = 1.381$$

*Carbide insert*
In the case of a carbide insert (hard metal) and a shrink ring of low alloyed steel, values according to Table 3 can be inserted in equation 7.10 resulting in a calculated interference.
$\Phi$ = 50 mm
$E_n$ = 580 000 N/mm$^2$, $\nu_n$ = 0.22
$E_a$ = 206 000 N/mm$^2$, $\nu_a$ = 0.296
If imposing a safety factor of 2 (i.e $S_1$=2), using equation 7.10 one gets:

$$\frac{I}{50} = \frac{200}{580000} \cdot \left\{ \frac{1+0.6^2}{2} \cdot 2 \cdot \left[ 2.125 - 0.22 + \frac{580000}{206000} \cdot (1381 + 0296) \right] - 1.125 \right\} = 0.00272$$

This means that I= 0.136 mm, which in turn means that the difference in diameters between the inner diameter of the ring and the outer diameter of the insert has to be 0.136 mm, i.e. $D_n$-$d_a$=0.136 mm. If one chooses $D_n$=50.045 mm corresponding $d_a$=49.909 since 50.045-49.909=0.136. Normally it is simpler to use all the interference on the shrink ring, i.e $d_a$=49.864.

In order to check if the strength of the shrink ring is sufficient the highest mutual pressure between the insert and the shrink ring is calculated according to equation 7.11.

$$P_m = E_n \cdot \frac{\left( \frac{I}{\Phi} + \frac{2 \cdot \alpha^2}{1-\alpha^2} \cdot \frac{P_i}{E_n} \right)}{\left[ \frac{1+\alpha^2}{1-\alpha^2} - \nu_n + \frac{E_n}{E_a} \cdot \left( \frac{1+\beta^2}{1-\beta^2} + \nu_a \right) \right]} \qquad \text{(eq. 7.11)}$$

All data needed in equation 7.11 is known from previous calculations. Inserted in equation 7.11 one gets:

$$P_m = 580000 \cdot \frac{\left( 0.00272 + 1.125 \cdot \frac{200}{580000} \right)}{\left[ 2.125 - 0.22 + \frac{580000}{206000} \cdot (1.381 + 0.296) \right]} = 272 \ \ N/mm^2$$

If no load is exerted upon the die, $P_i$=0 and the maximum stress is calculated according to equation 7.11 at 238 N/mm$^2$.
Once $P_m$(max) is calculated (in this case equated to 272 N/mm$^2$) it is possible to find the highest normal and transverse stress and check the maximum, ideal stress according to von Mises (eq. 7.11). This is made below for the shrink ring, which normally is the material with the lowest yield strength.

$$\sigma_r = -P_i \qquad \text{(eq. 7.12)}$$

$$\sigma_t = \frac{1+\beta^2}{1-\beta^2} \cdot P_1 \qquad \text{(eq. 7.13)}$$

$$\sigma_{vM} = \sqrt{\sigma_t^2 + \sigma_r^2 - \sigma_r \cdot \sigma_t} \qquad \text{(eq. 7.14)}$$

$$\sigma_r = -272 \;\; N/mm^2$$
$$\sigma_t = 1.381 \cdot 272 = 376 \;\; N/mm^2$$
$$\sigma_{vM} = \sqrt{376^2 + (-272)^2 - (-272) \cdot 376} = 564 \;\; N/mm^2$$

This stress level is well below the working limit of tool steels such as Uddeholms Orvar (corresponding to SS 2242 (Swedish standard), DIN 2344), where the yield strength is in the range of 1300-1600 N/mm$^2$.

*High speed steel insert*
The same calculations as for the hard metal in previous example can be made for a high speed steel insert. This means:
$d_n$ = 30 mm, $D_n$ = 50 mm, $d_a$ = 50 mm, $D_a$ = 125 mm
which of course gives the same values of $\alpha$ and $\beta$ as before. From Table 3 it is also clear that $E_n$ = 206 000 N/mm$^2$, $\nu_n$ = 0.296 and $E_a$ = 206 000 N/mm$^2$, $n_a$ = 0.296 and $E_n$ / $E_a$=1

Inserting these values in equation 7.10, and imposing $S_1$=2, one gets:

$$\frac{I}{50} = \frac{200}{206000} \cdot \left\{ \frac{1+0.6^2}{2} \cdot 2 \cdot \left[ 2.125 - 0.296 + 1 \cdot (1.381 + 0.296) \right] - 1.125 \right\} = 0.00354$$

$$\Rightarrow I = 0.177 \quad mm$$

Inserting the present values for calculations about the maximum mutual pressure, with equation 7.11, one gets:

$$P_m = 206000 \cdot \frac{\left( 0.00354 + 1.125 \cdot \frac{200}{206000} \right)}{\left[ 2.125 - 0.296 + 1 \cdot (1.381 + 0.296) \right]} = 272 \quad N / mm^2$$

The mutual pressure, "at rest", is when $P_i$=0, which results in $P_m$=208 N/mm$^2$.
Since $P_m$=272 N/mm$^2$ in the same way as for the hard metal insert one gets the same values for the ideal stress (equation 7.14).

### Compaction at 150°C

Calculations on a tool with the same nominal dimensions as before will be made for warm compaction.

*Carbide insert*
At 150°C values from Table 3 give:
$E_n$ = 555 000 N/mm$^2$, $\nu_n$ = 0.22 and $E_a$ = 196 000 N/mm$^2$, $\nu_a$ = 0.299 and
$E_n / E_a$=555 /196=2.832
$S_1$=2
$P_i$=200

The interference at 150°C is calculated according to equation 7.10:

$$\frac{I}{50} = \frac{200}{555000} \cdot \left\{ \frac{1+0.6^2}{2} \cdot 2 \cdot \left[ 2.125 - 0.22 + 2.832 \cdot (1.381 + 0.299) \right] - 1.125 \right\} = 0.00286$$

The calculated value represents the conditions at 150°C. In order to know the conditions at room temperature Bocchini et al [22] have proposed a method to calculate the ratio I/ϕ.

$$\left(\frac{I}{\Phi}\right)_{WC} = \left(\frac{I}{\Phi}\right)_{Tc} + \left(\left[\lambda_a - \lambda_n\right] \cdot \left[T_c - T_{R.T}\right]\right) \qquad \text{(eq. 7.15)}$$

where WC stands for warm compaction and Tc, compaction temperature, λ for the thermal expansion coefficient at compaction temperature for the insert (n) and the ring (a), Tc the compaction temperature and the other temperature for the room temperature. In this case, using the thermal expansion data from Table 3, it would result in:

$$\left(\frac{I}{\Phi}\right)_{WC} = 0.00286 + \left(\left[12.5 \cdot 10^{-6} - 5.5 \cdot 10^{-6}\right] \cdot \left[150 - 20\right]\right) = 0.00377$$
$$\Rightarrow I = 50 \cdot 0.00377 = 0.188 \ \ mm$$

The needed interference, I, at room temperature is thus 0.188 mm. Since the interference is bigger at room temperature and the stresses higher on the insert at rest, $P_i$=0 and all data at 20°C.
Put into equation 7.11 in order to equate the maximum mutual stress one gets:

$$P_m = 580000 \cdot \frac{0.00377}{\left[2.125 - 0.22 + \frac{580000}{206000} \cdot \left(1.381 + 0.296\right)\right]} = 330 \ \ N \ / \ mm^2$$

According to equations 7.12-7.14 the highest ideal stress is calculated:

$$\sigma_r = -330 \ N \ / \ mm^2$$
$$\sigma_t = 1.381 \cdot 330 = 456 \ \ N \ / \ mm^2$$
$$\sigma_{vM} = \sqrt{456^2 + (-330)^2 - (-330) \cdot 456} = 684 \ \ N \ / \ mm^2$$

*High speed steel insert*
At 150°C values from Table 3 give:
$E_n$ = 196 000 N/mm$^2$, $\nu_n$ = 0.299 and $E_a$ = 196 000 N/mm$^2$, $\nu_a$ = 0.299
$E_n / E_a$ =196/196=1
$S_1$=2
$P_i$=200

According to equation 7.10 one gets:

$$\frac{I}{50} = \frac{200}{196000} \cdot \left\{ \frac{1+0.6^2}{2} \cdot 2 \cdot \left[ 2.125 - 0.299 + 1 \cdot \left( 1.381 + 0.299 \right) \right] - 1.125 \right\} = 0.00372$$

The value has to be corrected because of the temperature according to equation 7.15:

$$\left( \frac{I}{\Phi} \right)_{WC} = 0.00372 + \left( \left[ 12.5 \cdot 10^{-6} - 9.5 \cdot 10^{-6} \right] \cdot \left[ 150 - 20 \right] \right) = 0.00411$$
$$\Rightarrow I = 50 \cdot 0.00411 = 0.205 \ \ mm$$

The highest mutual stress at rest, as in the case with the carbide insert,$P_m$ is equated according to equation 7.11:

$$P_m = 206000 \cdot \frac{0.00411}{\left[ 2.125 - 0.296 + 1 \cdot \left( 1.381 + 0.296 \right) \right]} = 242 \ \ N / mm^2$$

Resulting in according to equation 7.12-7.14:

$$\sigma_r = -242 \ N / mm^2$$
$$\sigma_t = 1.381 \cdot 242 = 334 \ \ N / mm^2$$
$$\sigma_{vM} = \sqrt{334^2 + (-242)^2 - (-242) \cdot 334} = 501 \ \ N / mm^2$$

**Summary of calculations**

The calculations in previous sections show that there are differences with various materials and different temperature conditions when shrink-fitting an insert in a ring. The calculated data are summarized in Table 4 below.

**Table 4.** Summary of the calculated values (only valid for the present dimensions)**.**

| | Hard metal insert | | High speed steel insert | |
|---|---|---|---|---|
| Temperature,°C | 20 | 150 | 20 | 150 |
| Interference, mm | 0.136 | 0.188 | 0.177 | 0.205 |
| Maximum ideal stress, $N/mm^2$ | 564 | 684 | 564 | 501 |

## 7.6 Different ways of heating, cooling and insulation

As has been discussed, a uniform, symmetrical temperature distribution is important for the clearances and tolerances of the tooling. That is also very important for the columns in the tool set for instance. If one column has another temperature than the others it will change its dimensions and create tensions and, in the end, perhaps distort the upper punch plate.

Two completely different strategies have been tested when it comes to temperature distribution in the tool set: heating the whole set and heating only the parts that have to be heated due to contact with the powder.

In the first case the rest of the press has to be protected only at the connecting points between tool set and press by cooling and/or insulation, and in the second case cooling has to be made within the tool set. Because of the energy demands in the first case – heating the whole tooling set – strategy number two has been proven more successful. The next figure shows the tool set and the areas that have to be warm and those that have to be "cold" according to the second heating strategy. See figure 27 on page 63.

### Temperature settings for Densmix™

Usual temperature settings for Densmix™ are powder at 130°C and tool at 150°C, as with many examples shown in this book. These settings in turn demand a certain temperature distribution in the warm areas in the tool set, as shown in figure 27.

The flowability of powder begins to dramatically change if the temperature exceeds 130°C by more than just a few degrees (see figure 7 in section 4). In order to ensure a consistent powder flow, the adaptor table is heated only at the rear-end position of the moving filling shoe (i.e. at the position for filling from the stationary feeder). Heating is generated from underneath the adaptor table, giving a maximum 130°C on its surface; the adaptor table is not heated in any other location. In fact, it is often insulated to ensure it does not exceed 130°C due to heat transfer from the die. The upper punch is heated to 150°C with a band element (or in some cases, cartridge heater/s), controlled by a thermocouple. The lower punch is provided with heat from the die. It is actually only the surfaces that have contact with the powder which must be kept at the right temperature (i.e. maximum 130°C on the adaptor table; 150°C on the surfaces of the upper and lower punch and the die).

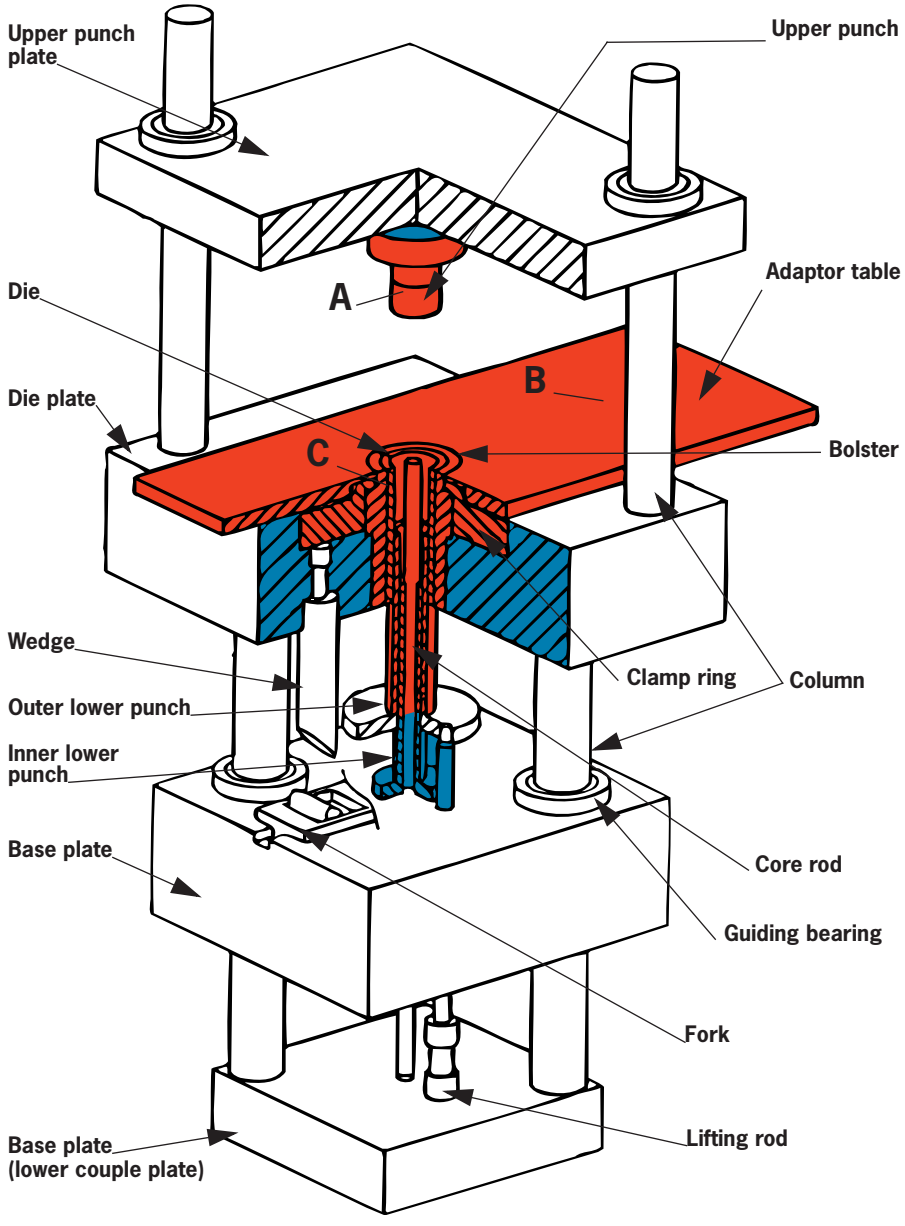


*Figure 27. Heating (red), cooling and insulation (blue) on the tool set for warm compaction. A - C: areas/zones with controlled heating. In the case of Densmix™ generally: A + C =130°C - 150°C, B=125°C - 130°C.*

In theory it should be sufficient to insulate the boundaries between the temperature zones if conduction was the only heat transport mechanism at work. Because of thermal radiation and heated air due to convection between parts in the tool set, cooling is necessary in most cases.

In the case of a simplified adaptor, cooling with cooling flanges/gills, together with insulation is sufficient. See figure 28.

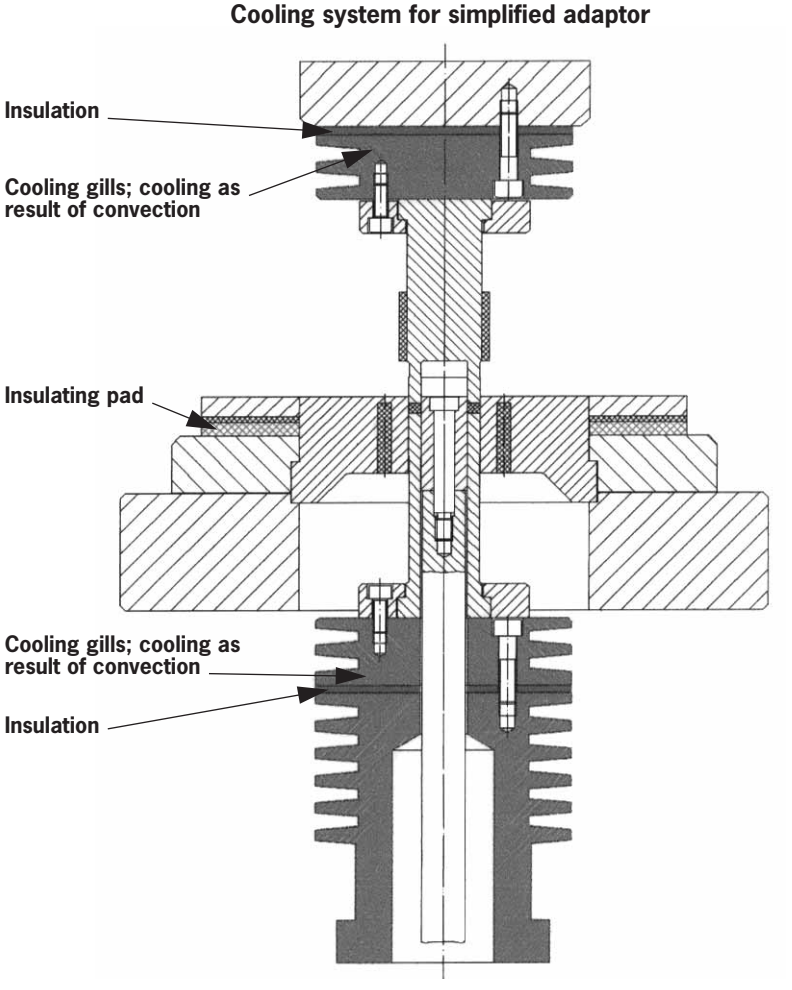


*Figure 28. Cooling system for simplified adaptor (Published with the permission of Alvier AG).*

Heating for the same tooling as in figure 28, is shown in figure 29.

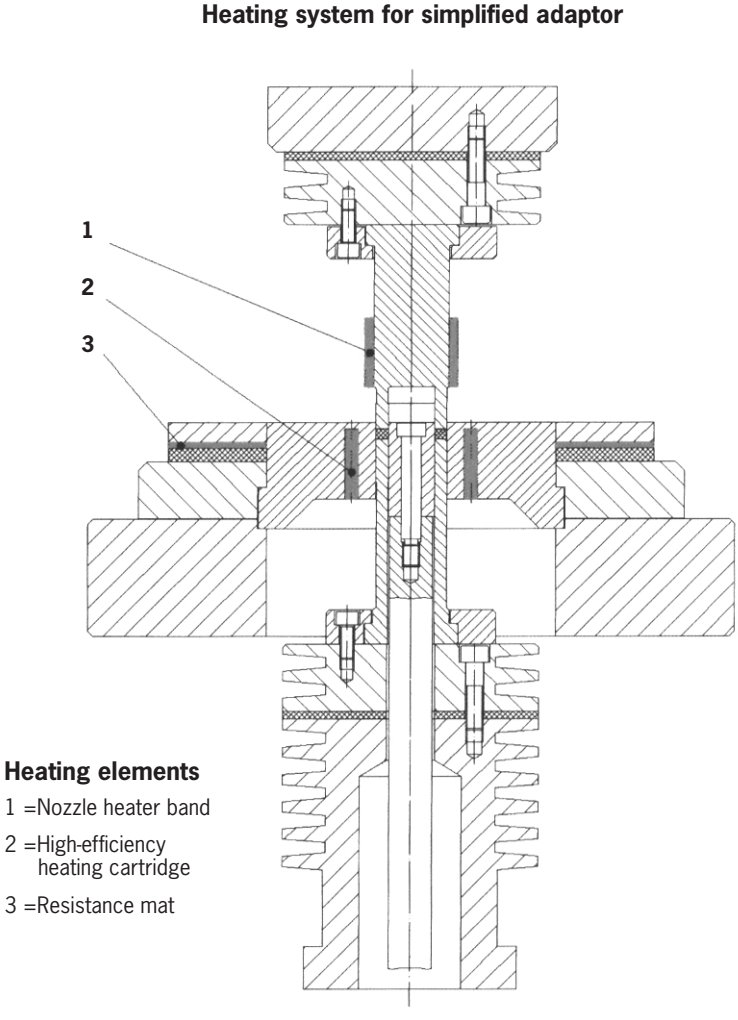


*Figure 29. Heating system for simplified adaptor (Published with the permission of Alvier AG).*

The most common way of heating the die is to use cartridge heaters inside the die, whilst in the case of the upper punch, band elements are recommended. If the upper punch has a complex geometry a spacer for the band elements has to be made, or in some cases

cartridge heaters are even placed inside the punch. The adaptor table is heated by foil elements. Holes for the cartridge heaters should be made so that the tip of the heaters are as close as possible to the top of the die.

Cartridge heaters should be connected in parallel and the temperature controlled by a thermocouple positioned at a distance of ~ 15 mm, centre to centre, to one of the cartridges and preferrably at half the length/height.

A cooling system for a multi-platen adaptor from Alvier AG is presented, showing a more complex situation than in the other figures. See figure 30 on page 67. Similary, a heating system for a multi-platen adaptor from Alvier AG is presented, showing a more complex situation than in the other figures. See figure 31 on page 68.

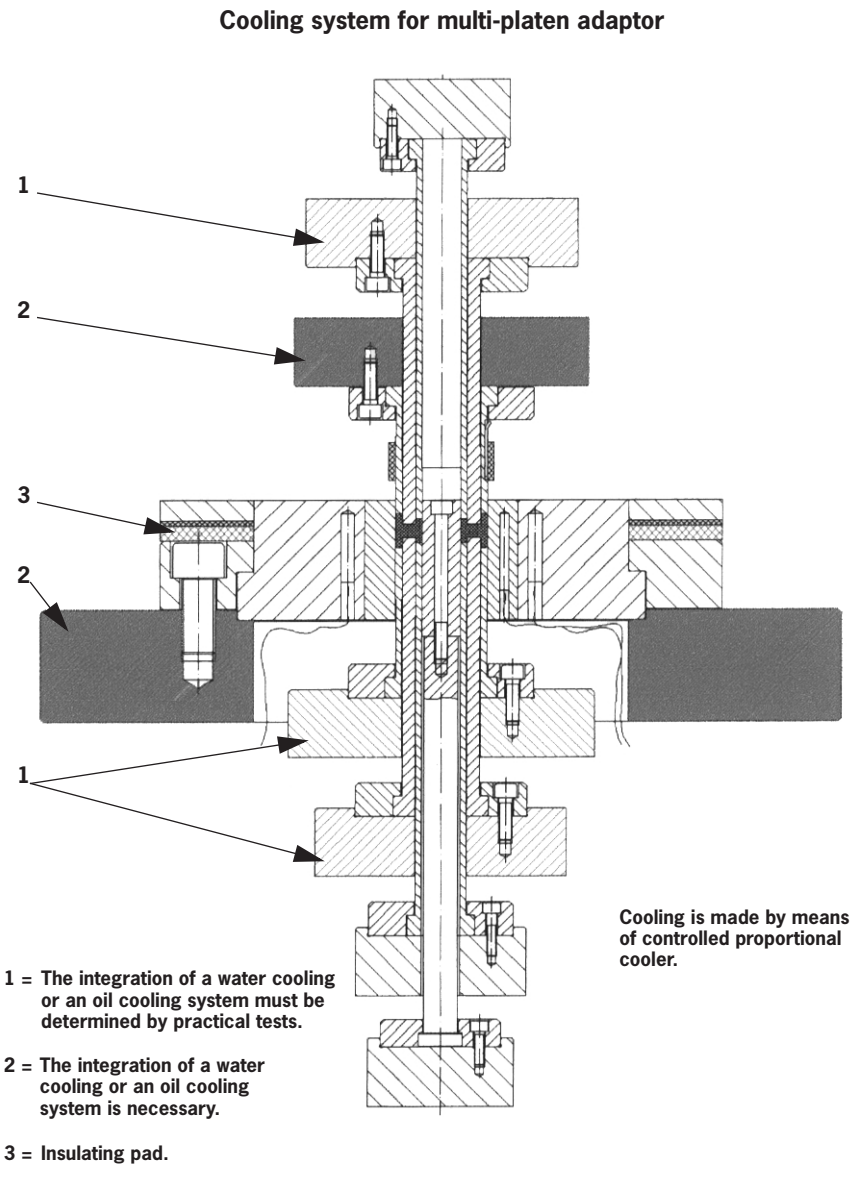


*Figure 30. Cooling system for multi-platen adaptor. (Published with the permission of Alvier AG.)*

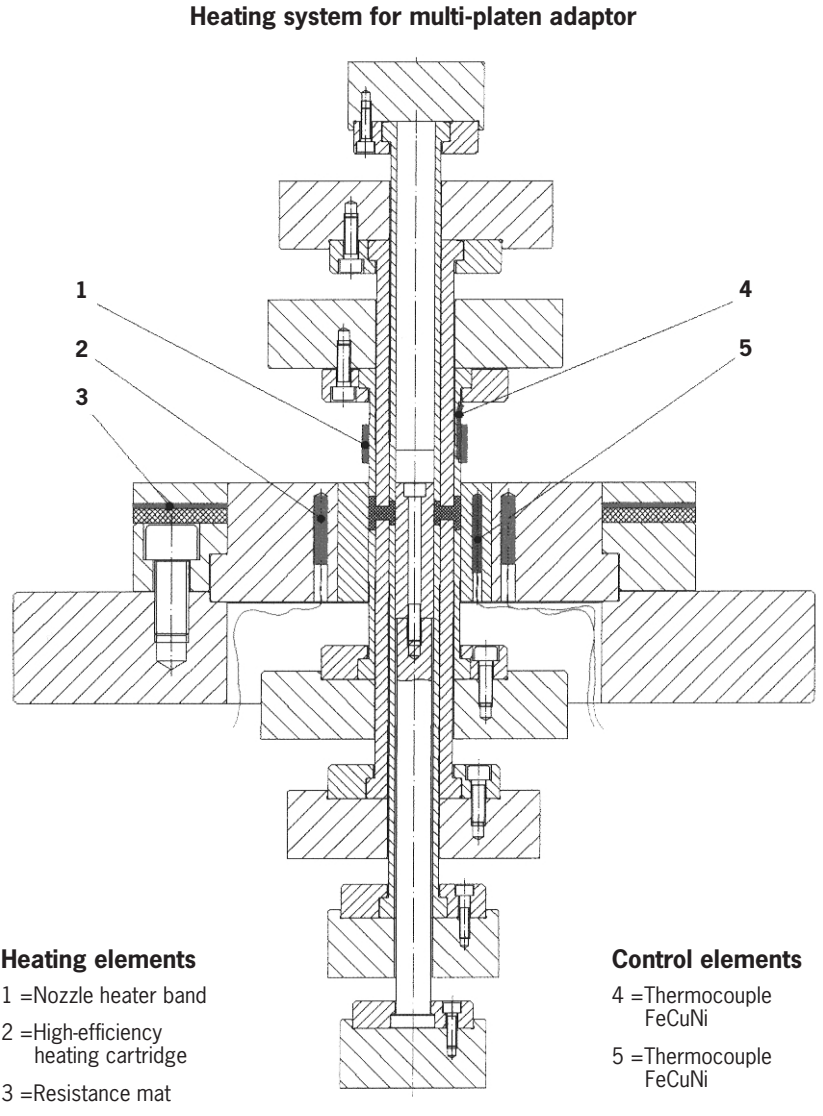


*Figure 31. Heating system for multi-platen adaptor. (Published with the permission of Alvier AG.).*

## 7.7 Tool materials

There are no special demands on materials for construction of tools for warm compaction, compared with cold compaction. The most important differences relate to clearance and shrink fit (as dealt with in sections 7.4 and 7.5)

Materials with very stable and even thermal expansion are recommended, since they are homogeneous and isotropic, regardless of their (average) chemical composition. These requirements are well met by using high speed steels. Of course the materials must have the right levels of hardness and strength.

Combinations of materials with different thermal expansions require special attention. (See figure 32 for examples of various materials and their application in a warm compaction tool). In zones with high tolerances, abrasion and stresses, carbide or high speed steel is required, while in zones without such high demands, a simpler (i.e. cheaper) steel is usually appropriate.

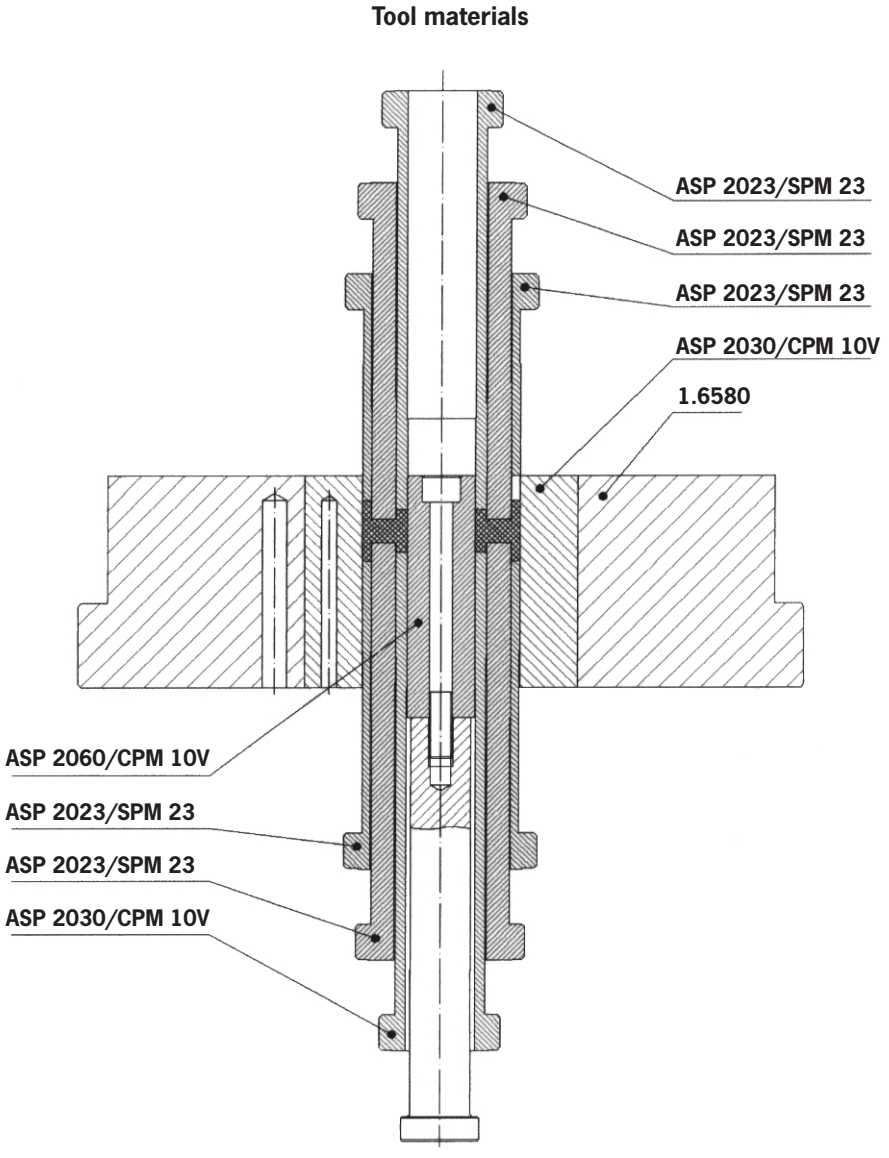


*Figure 32. Tool materials in a steel tool for warm compaction, (Published with the permission of Alvier AG.)*

# 8 Dewaxing

The powder currently available for warm compaction (Densmix™ from Höganäs AB) normally has a lubricant content of 0.6%. The organic content consists of a more complex chemistry than traditional lubricants as it is especially designed for working at elevated temperatures.

This chapter is mainly focused on the following topics:

- Dewaxing process.
- The density influence.
- Blisterings.
- Stains and discolourisations.

Experiences with dewaxing and sintering have so far been very good. General guidelines for sintering and dewaxing are also applicable for warm compaction. Dewaxing and the influence of densities is covered in two seperate sections in this chapter.

## 8.1 Dewaxing process

Dewaxing has been characterised through the Thermo Gravimetric Analyse system (TGA) in which the weight difference is recorded during the temperature increase. In next figure the dewaxing process is described for Distaloy AE (processed as Densmix™) and the weight difference is recorded at a temperature gradient of 50°C/min in a gas mixture of 96% $N_2$ /4% $H_2$, in order to simulate dewaxing in an ordinary production furnace. See figure 33.

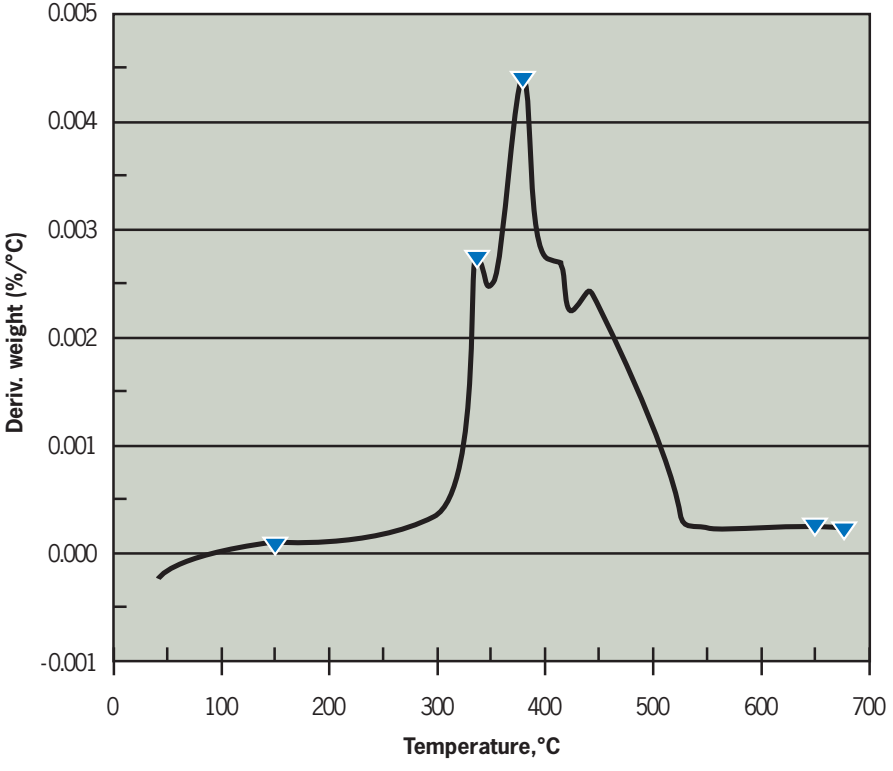


*Figure 33. The dewaxing characteristic for Distaloy AE Densmix™ at a heating rate of 50°C/minute. The curve shows the time derivative of the weight change curve (dm/dt).*

As seen in the figure, the dewaxing process takes place in the temperature interval between 300-550°C and the largest weight loss was recorded at about 400°C.

The dewaxing is considered complete at 700°C, as has been seen in fractography studies of dewaxed samples. After dewaxing at 700°C no signs of remaining organic substances can be detected.

Lower temperature gradient (i.e. the rate of temperature increase) will push the dewaxing interval towards 250-500°C, when the dewaxing is performed in better thermal equilibrium. The dew point has not been observed to have any influence on the dewaxing rate.

## 8.2 The influence of density

Through warm compaction technology, densities up to 99 % of full theoretical density can be reached. The dependency of the dewaxing on the density has been studied in TGA and according to those results the density does not influence the dewaxing between 91 to 99 % of full theoretical pore free density. See figure 34. The diagram shows that the temperature interval remains in principle unaffected for the density interval.

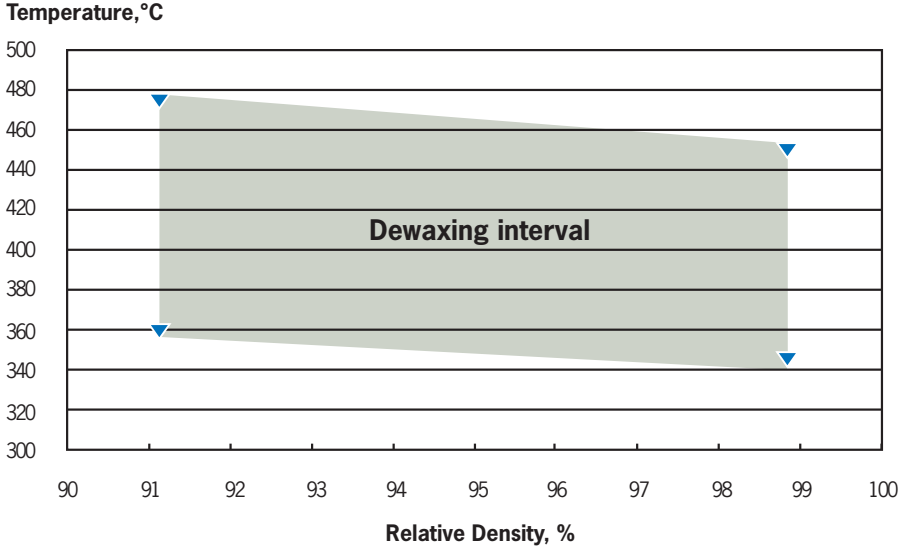


*Figure 34. The dewaxing temperatures for Densmix™ as a function of the relative density.*

## 8.3 Blistering

The organic content in Densmix™ behaves somewhat the same as Amide wax during dewaxing. It does not have to decompose inside the component and therefore the blistering tendency is reduced immensely. Trials with an initial temperature rise of about 350°C/minute for components with a density of 7.25 g/cm$^3$ did not give any problems with blisterings or pop corning. Furthermore, neither the mechanical properties nor the pore structure were affected due to the very rapid temperature increase. Therefore the blistering tendency is considered negligible for warm compaction.

## 8.4 Stains and discolourisations

Stains and granular soot have been observed after sintering, but they can be avoided. In order to avoid stains and discolourisations on the surface some general guidelines can be given.

- A higher driving force by means of a higher temperature gradient (at least 50°C/min) will diminish the problem when dewaxing.
- An atmosphere with hydrogen is favourable and the more hydrogen the better.
- The dew point does not seem to affect the formation of stains.
- A counter-current gas-stream (opposite the direction of the material) will diminish the problem.

# 9 Pressed and sintered properties

This section will give examples of different material systems and their as-pressed (green) properties and as-sintered properties. Comparison with other compaction methods such as conventional “cold” (1P1S) and double press and sintering (2P2S) will also be made.

## 9.1 Green properties

### Green Densities

As mentioned earlier green densities are increased with warm compaction compared to conventional. A comparison between conventional and warm compaction has been made on two materials. It is seen that a density increase of approximately 0.10-0.30 g/cm$^3$ is achieved (iron powder based materials). See figure 35.

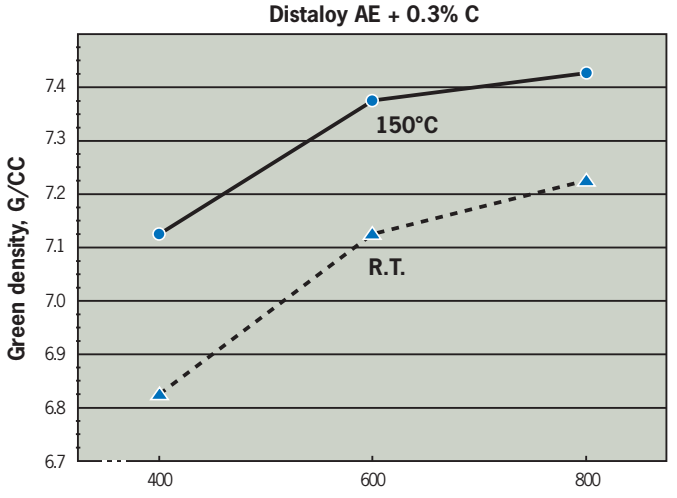


Influence of compaction temperature on green density of Distaloy AE+0.3% C

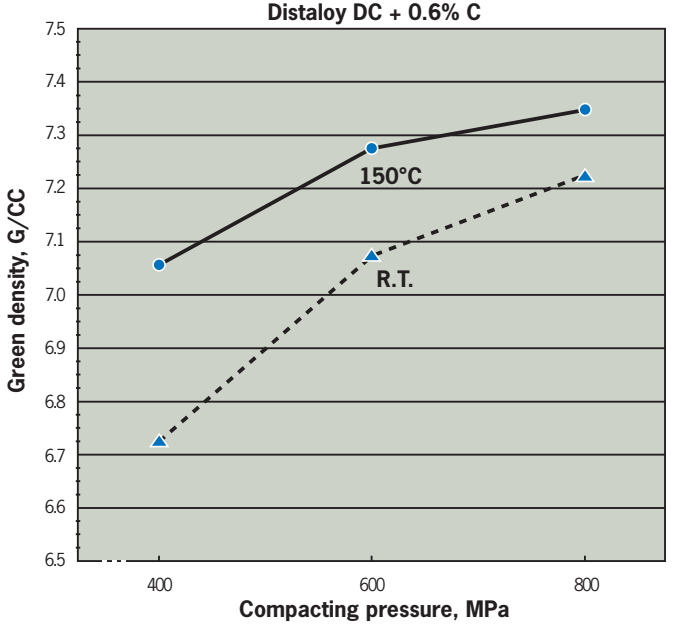


Influence of compaction temperature on green density of Distaloy DC+0.6% C

*Figure 35. Green density for two different materials as a Densmix™, compacted at room temperature and at 130/150°C powder/tool temperature.*

### Pore Free Densities

One of the differences with warm compaction in relation to conventional, "cold", is that the higher density levels achieved (lower porosity levels), are closer to the maximum pore-free density of the green compact, also known as the theoretical density of the mix.

Further pressing at higher pressures in order to reach higher densities, in these situations, will damage the compact and the die. Table 5, below, shows the pore-free densities measured with pycnometry and the inverted value, specific volume, of some standard grades of iron and steel powders and additives. LUBE below denotes the binder/lubricant system used in a Densmix™.

**Table 5.** Approximated pore-free densities of some standard grades and additives.

| Material | Theoretical density ρ (g/cm$^3$) | Theoretical specific volume 1/ρ (cm$^3$/g) |
|---|---|---|
| ASC100.29 | 7.83 | 0.128 |
| ABC100.30 | 7.83 | 0.128 |
| NC100.24 | 7.75 | 0.129 |
| SC100.26 | 7.76 | 0.129 |
| Distaloy AE | 7.88 | 0.127 |
| Distaloy AB | 7.86 | 0.127 |
| Astaloy Mo | 7.85 | 0.128 |
| Ni | 8.84 | 0.113 |
| Cu | 8.90 | 0.112 |
| Graphite UF-4 | 2.28 | 0.439 |
| Graphite F-10 | 2.25 | 0.444 |
| LUBE | 1.03 | 0.971 |
| MnS | 3.86 | 0.259 |

The theoretical density for a certain mix is achieved by adding the masses of the different mix components divided by the sum of the volume of each component expressed by equation 9.1. Where $m$ is the mass of each component and $V$ the volume:

$$\rho_t = \frac{m_1 + m_2 + \ldots\ldots\ldots m_n}{V_1 + V_2 + \ldots\ldots\ldots V_n} = \frac{\sum m}{\sum V} \qquad \text{(eq. 9.1)}$$

A simpler way is to define the mass fraction - the content of each component in weight percent divided by 100 - and multiply each mass fraction with corresponding specific volume (or divide by density). The theoretical pore free density is then the added, inverted, value. If *x* denotes the mass fraction, the theoretical pore free density is achieved with the following equation:

$$\frac{1}{\rho_t} = \frac{x_1}{\rho_t^1} + \frac{x_2}{\rho_t^2} + \ldots\ldots \frac{x_n}{\rho_t^n} = \sum_{i=1-n} \frac{x_i}{\rho_t^i} \qquad \text{(eq. 9.2)}$$

**Example 1**
What is the theoretical pore free density of a Densmix™ containing,
Distaloy AE + 0.3% C-UF + 0.6% LUBE ?

$X_1$ = 0.003, Graphite
$X_2$ = 0.006, LUBE
$X_3$ = 1 - $X_1$ - $X_2$ = 0.991, Distaloy AE

$\rho^1{}_t$ = 2.28 g/cm$^3$, from table 3.
$\rho^2{}_t$ = 1.03 g/cm$^3$, from table 3.
$\rho^3{}_t$ = 7.88 g/cm$^3$, from table 3.

Using equation 9.2 the solution is:

$$1/\rho_t = \frac{0.003}{2.28} + \frac{0.006}{1.03} + \frac{0.991}{7.88} = 0.133 \text{ cm}^3/\text{g} \quad \Rightarrow \quad \rho_t = \frac{1}{0.133} = 7.52 \text{ g/cm}^3$$

The answer is: **7.52 g/cm$^3$**

The above value means that the highest achievable green density is 7.52 g/cm$^3$ for this specific mix.

**Green Strength**
As has been shown in section 4, the green strength is significantly increased with warm compaction compared to conventional, “cold”. See figure 36 on page 79. The figure shows a comparison between different mixes compacted at room temperature and at elevated temperature. Materials compacted at elevated tool temperature were prepared according to the Densmix™ concept with 0.6% lubricant, and mixes compacted at room temperature were conventionally mixed and lubricated with 0.8 % Zn-stearate.

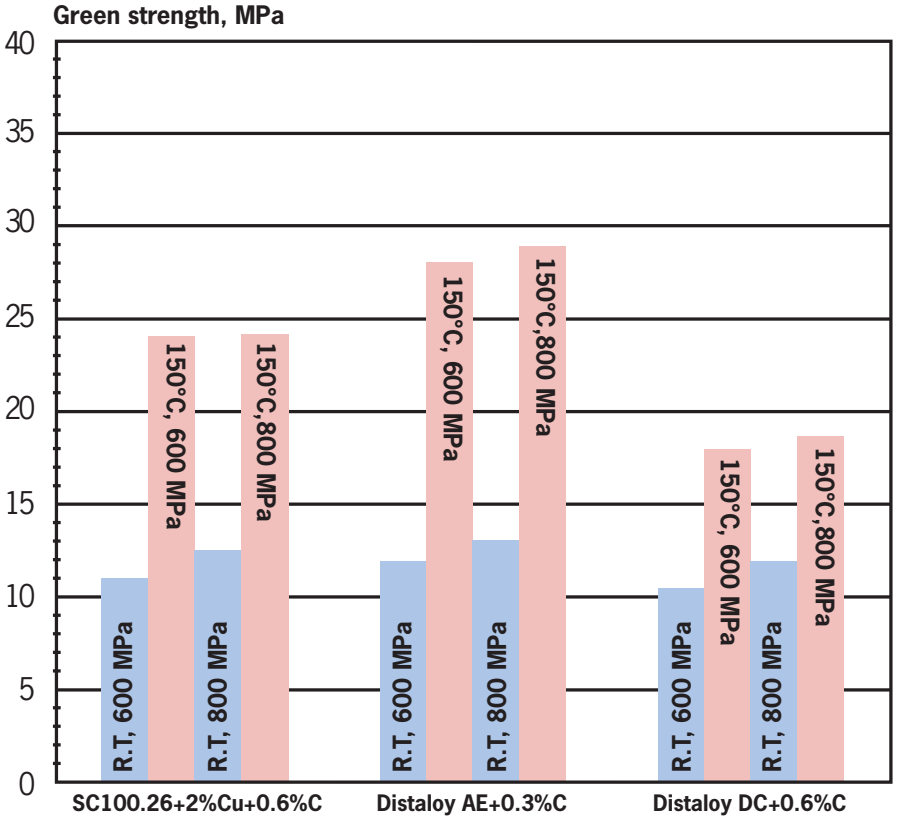


*Figure 36. Comparison of green strength for different P/M materials after compaction at 150°C tool temperature and 130°C powder temperature and at room temperature. Trials on a 45 ton mechanical Dorst press.*

Above shown effect is not a function explained by the higher densities for the warm compacted specimens as is shown below. See figure 37 on page 80. The green strength is significantly higher for the warm compacted parts regardless of density. See also the theoretical density as calculated in Example 1, above.

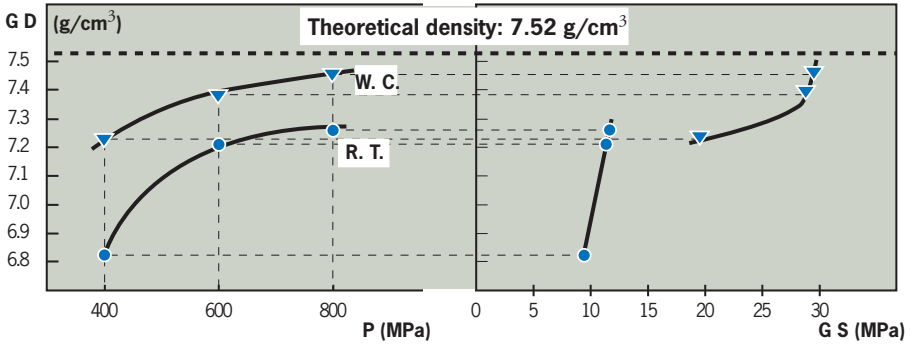


*Figure 37. Green density as a function of pressure and green strength for two mixes: Densmix™ (Distaloy AE + 0.3% C + 0.6% lubricant) compacted at 150°C tool temperature and 130°C powder temperature (W. C.), compared with a conventional "cold" mix (of the same nominal components) compacted at room temperature (R. T.).*

## Spring back

The radial green expansion that takes place when a component is ejected from a die, is normally denoted as spring back. Green expansion characteristics for Distaloy AE + 0.3% C, as a Densmix™, compacted at different temperatures and tool materials are compared in the next figure. See figure 38.

Radial green expansion is lower for the warm-compacted powder than for the conventional compacted powder. At higher densities (at compaction pressure of 800 MPa) green expansion is increased but still lower than for compacting at room temperature.

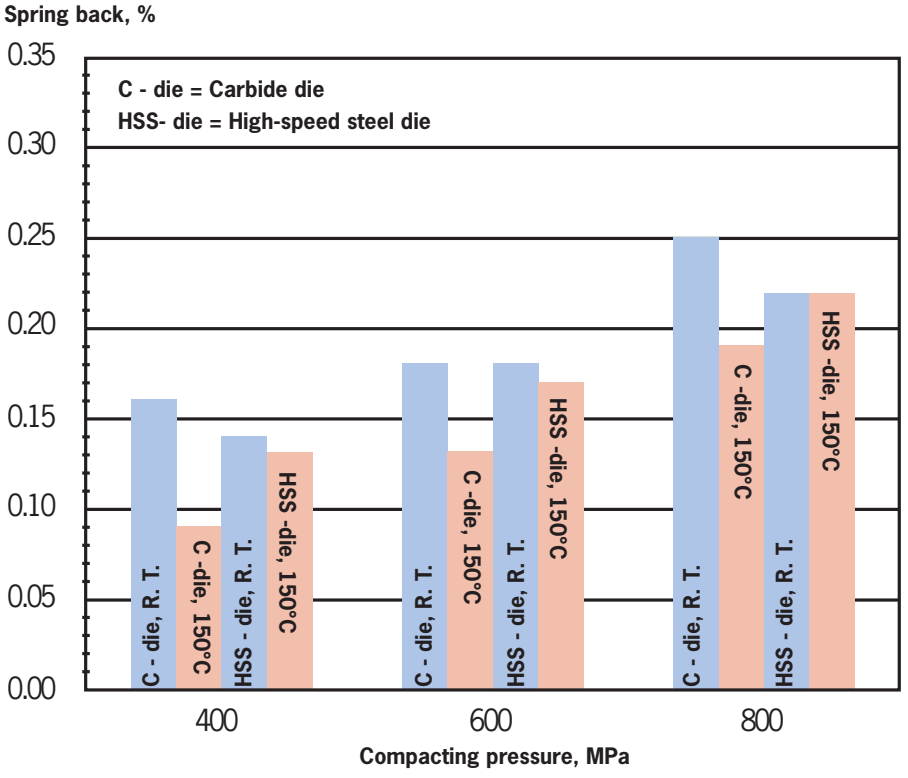


*Figure 38. Spring back for Distaloy AE + 0.3% C in different die materials after compaction at 130/150°C and room temperature. All measures made at R.T.*

## 9.2 Sintered properties

### Density

Not only the green density is affected, but also the sintered. Below it is clearly seen that the density level is still increased after sintering as well as after pressing. See figure 39.

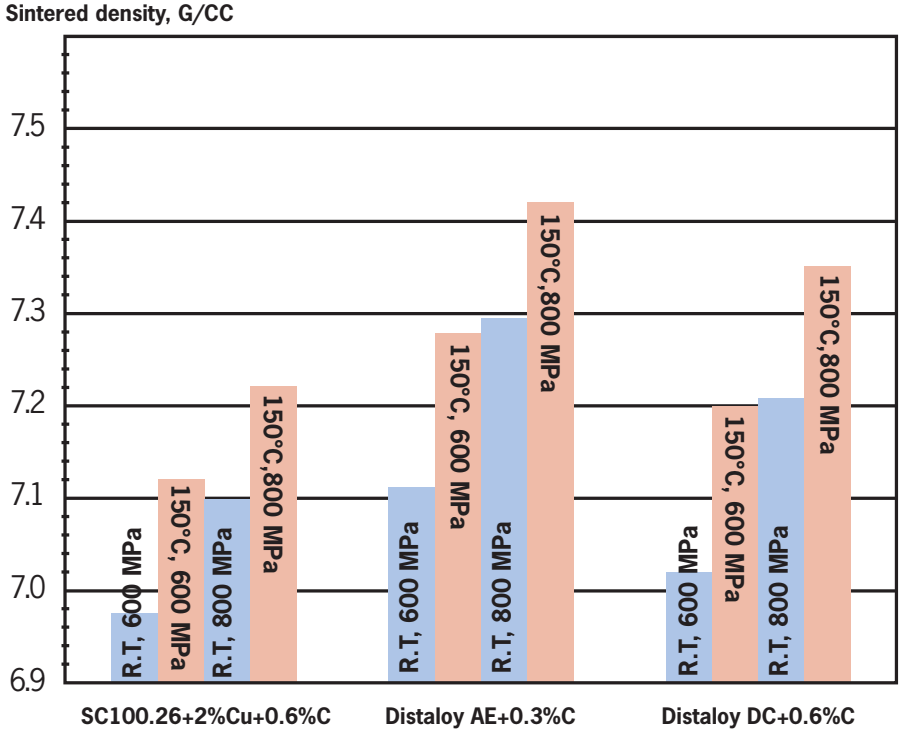


*Figure 39. Sintered density of different P/M materials after compaction at room temperature and 130/150°C powder/tool temperature. Sintering at 1120°C for 30 minutes in Endogas with carbon potential corresponding to the nominal carbon composition in the mix.*

### Dimensional change

The dimensional change level has an impact on the tolerances, or the scatter of dimensional change. This is well known and reported already 1976 [15], and is also the reason why "zero-growth" powders were developed by Höganäs AB.

Dimensional changes are also affected by the temperature increase. TS-bars according to standard measures, were pressed in an automatic hydraulic press, of two different materials mixed as a Densmix™:

- Material 1: Distaloy AE + 0.3% C + 0.6% Lubricant.
- Material 2: Astaloy 85 Mo + 0.3% C + 0.6% Lubricant.

Axial pressures of 500, 600, 700 and 800 MPa and powder temperatures/tool temperatures of 50/50, 100/100 and 130/150°C were used.

Before sintering in 90%$N_2$/10%$H_2$ with 0.3% corresponding carbon potential at 1120°C for 20 minutes, the length of the TS-bars were measured. After sintering the same dimensions were measured. See figure 40 on page 84. The result of this treatment, as can be seen with material 2; the fully prealloyed 0.85% Mo-material shows more shrinkage at higher densities whilst the Distaloy™ material is more stable. A slight increase in the dimensions of material 2 can be observed at increasing density. Generally a temperature raise will move the dimensional change curve up in the diagram, almost parallel, giving less shrinkage of the material.

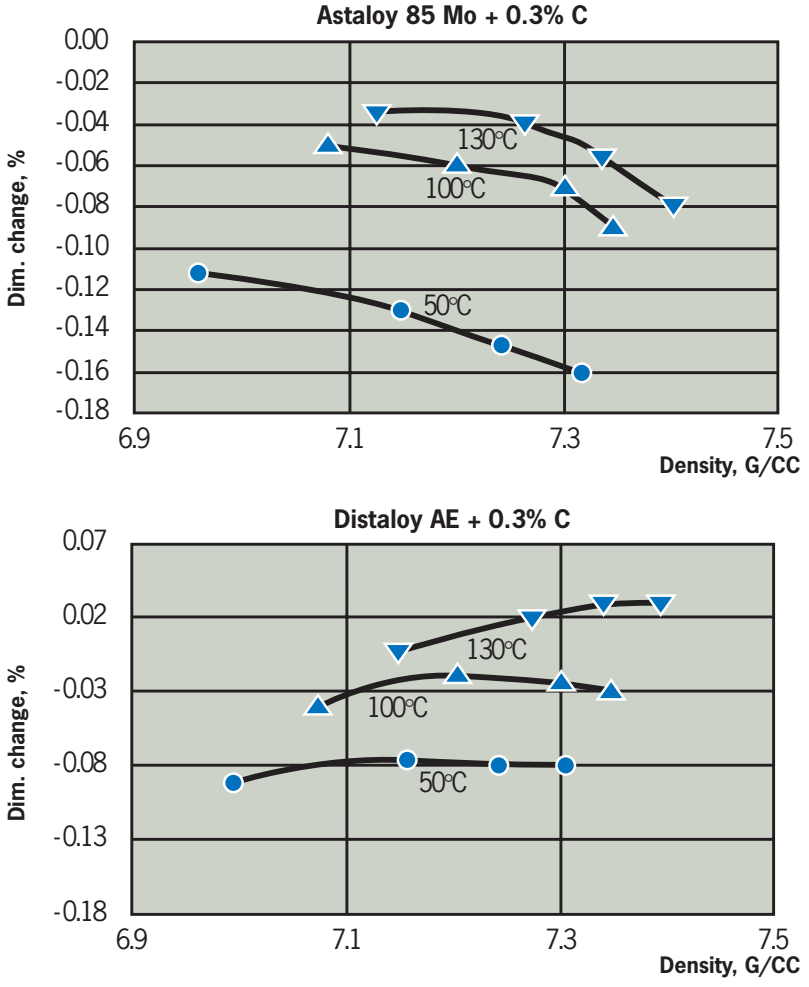


*Figure 40. Comparison of dimensional change (green – sintered state) of two mixes prepared as a Densmix™ compacted at 50/50, 100/100 and 130/150°C powder/tool temperature, pressing at 500, 600, 700 and 800 MPa, TS-bars, floating die, with 50 MPa axial load during ejection. Sintering in 90 % $N_2$/10% $H_2$ with controlled carbon potential at 1120°C for 20 minutes.*

**Tensile properties**

Tensile strengths for three different materials are shown in the next figure. See figure 41. As can be seen the tensile strength has increased about 10-15% for all materials, where the tensile properties of the warm compacted mixes at 600 MPa pressure are at the same level as for conventional compaction at 800 MPa. This effect corresponds well to the density increase of the material shown above.

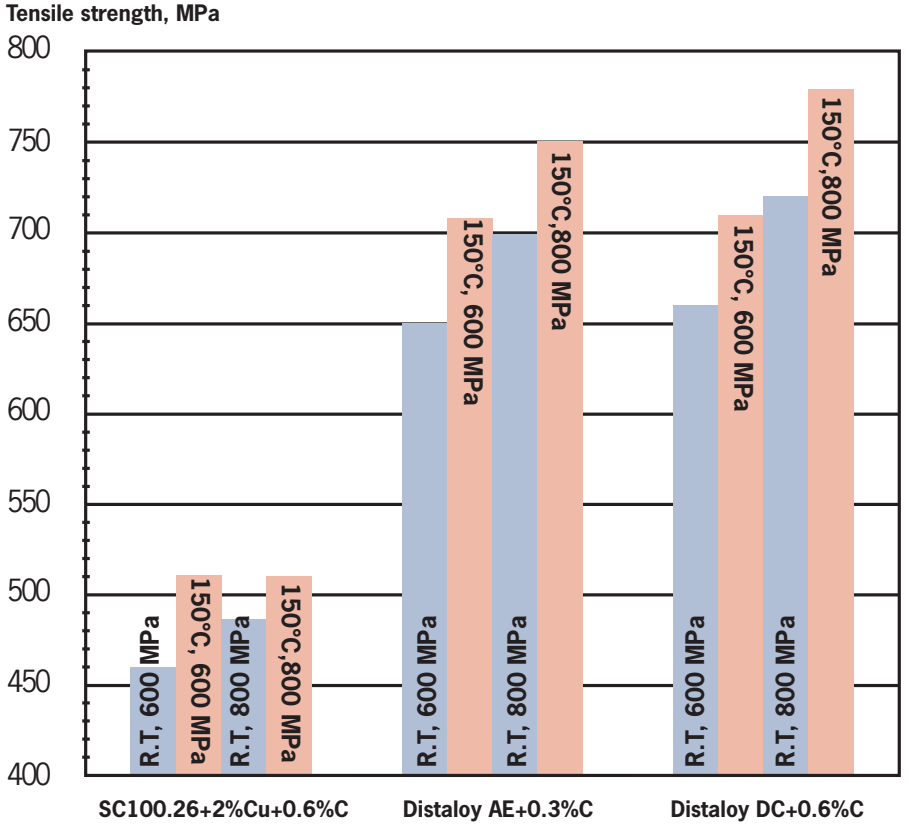


*Figure 41. Comparison of tensile strengths of different P/M materials compacted at room temperature and at 130/150°C powder/tool temperature, two different pressures. Sintering at 1120°C for 30 minutes in endogas with carbon potential corresponding to the nominal carbon composition in the mix.*

**Fatigue properties**

Fatigue properties are also influenced in a positive way by warm compaction. In the following test the bending fatigue strengths for two Distaloy™ materials with an admixed carbon content of 0.5%, are compared at the same density obtained by warm compaction and by conventional double pressing and double sintering (2P2S), and with cold compaction of the same nominal mixes compacted at a fairly standard pressure.

The powder for cold compacting, 1P1S, was admixed with 0.5% C and 0.6% Kenolube™, compacted at 600 MPa, sintered in endothermic gas at 1120°C for 30 minutes giving a density of approximately 7.1 g/cm$^3$.

The warm compacted specimens were compacted at 700 MPa to obtain a density in the range of 7.35-7.40 g/cm$^3$. Sintering was carried out at 1120°C for 30 minutes in endothermic atmosphere with controlled carbon potential.

In the case of double press and sintering (2P2S) the first pressing was carried out at 700 MPa and the second pressing at 500-550 MPa, depending on the powder. Cold compaction was carried out with 0.6% Kenolube™ admixed as a lubricant. Presintering was carried out at 750°C for 20 minutes in 90/10 nitrogen/hydrogen atmosphere for both materials. Final sintering was carried out at 1120°C for 30 minutes.

Sintered densities of the test specimens are presented below in figure 42.

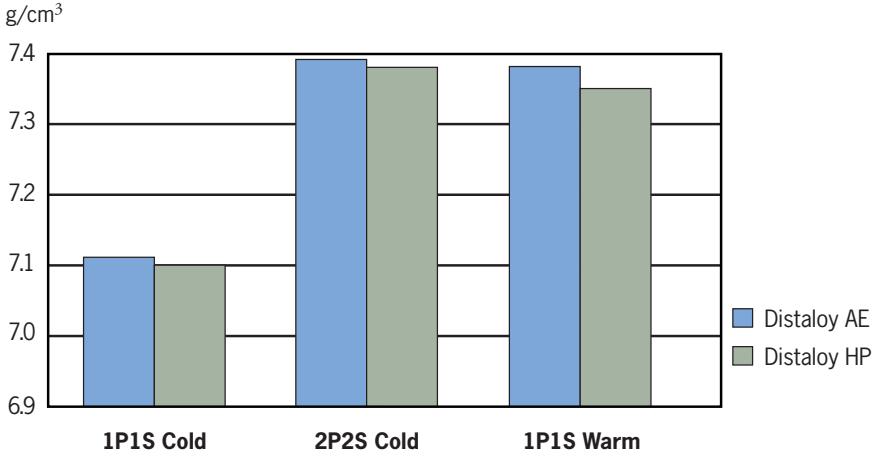


*Figure 42. Sintered densities in g/cm$^3$ of the two Distaloy™ materials, with 0.5% C, processed at different conditions.*

Unnotched fatigue test bars were tested in plane bending mode with an R value of -1. The results of these tests are shown in figure 43 below.

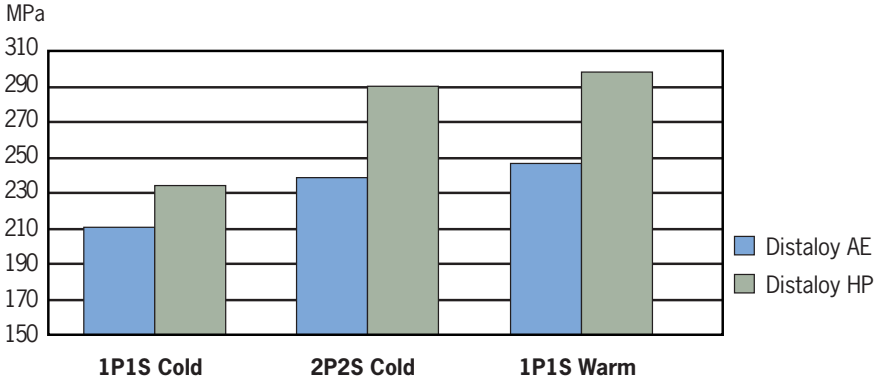


*Figure 43. Plane bending fatigue results in MPa of two different Distaloy™ materials with an admixed carbon content of 0.5%.*

As can be seen the fatigue strength has increased in the case of double press and sintering and warm compaction compared to 1P1S. The major influence is the higher achieved density, in the case of Distaloy AE going from 7.11 to 7.38-7.39 g/cm$^3$ and, in the case of Distaloy HP, from 7.10 to 7.35-7.38 g/cm$^3$. The lower impact on density with the Distaloy HP-material is due to the solid solution strengthening of the base-powder in this mix consisting of a fully pre-alloyed Fe-1.5% Mo-alloy, resulting in a higher deformation resistance.

It is interesting to note that the warm compacted specimens show a slightly higher fatigue strength than the ones compacted with double press and double sintering. This is not a function of density since the density of the 2P2S specimens and the warm compacted specimens are approximately the same. A plausible explanation is found in the pore structure where the maximum pore length is one determining factor. It has been shown several times [5,16] that the maximum pore length is decreased with warm compaction. The maximum pore length is determining the dynamic properties in the absence of other (larger) defects.

In next figure two micrographs of the pore structure are seen at approximately the same average density level. See figure 44 on page 88.

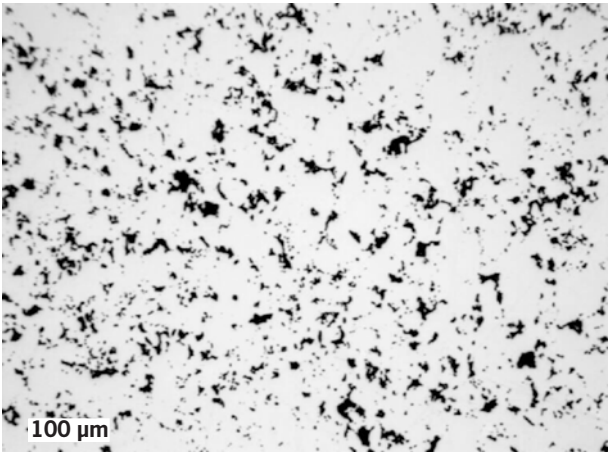


(a)
Densmix™
Distaloy AE+0.3% C

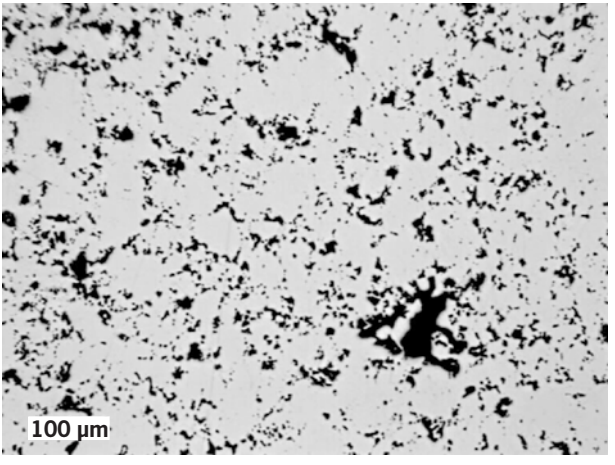


(b)
Amide wax
Distaloy AE+0.3% C

*Figure 44. Micrographs of P/M mixes. Composition: Distaloy AE + 0.3% C.*
*The* warm compacted *(a) specimen: 600 MPa, 130/150°C powder/tool temperature, 7.27 g/cc average density, prepared as a Densmix™.*
*The* cold compacted *(b) specimen: 800 MPa, 7.29 g/cc av. density, Premix (0.6% Amide wax).*

*Sintered in 90% $N_2$/10% $H_2$ atmosphere with controlled carbon potential at 1120°C for 20 minutes. Compacted TS-specimens in automatic press, floating die, 50 MPa axial pressure during ejection.*

# 10 Practical experiences

This section gives information about problems that can occur when installing and working with warm compaction. If identified before installation, it is easy to avoid problems. The practical experiences are based on working with Slot Heater systems.

**Table 6.** List of general problems.

| Heat-exchanger | Cone | Hose | Filling shoe | Die | Component |
|---|---|---|---|---|---|
| 1. No powder flow into the cone. See page 90. | 1. No powder flow into the cone. See page 91. | 1. No powder flow into the filling shoe. See page 92. | 1. Uneven temperature of the powder. See page 93. | 1. Uneven temperature distribution. See page 95. | 1. Inconsistency in weight, height and density of compacts. See page 97. |
| 2. Powder leakage during deadlock. See page 90. | | | 2. Arch formation See page 94. | 2. Overheating. See page 95. | 2. Lamination cracks in pressed components. See page 97. |
| 3. Oil leakage at the oil heater during deadlock. See page 90. | | | | 3.The die insert popping out during compaction. See page 95. | |
| | | | | 4. Scoring between die and punches or burr on the components. See page 96. | |
| | | | | 5. High friction between adaptor plates and columns. See page 96. | |

## 10.1 Heat Exchanger

**Heat exchanger:** No powder flow into the cone (valve does not open).

| Cause | Recommended actions |
|---|---|
| Too low air-pressure. | Check the pneumatic system. |
| Level sensor not sensitive enough. | Adjust according to user's manual (Linde). Clean the sensor. |
| Failure of the level sensor. | Check electrical connections, repair, exchange. |

**Heat exchanger:** No powder flow into the cone (arch formation).

| Cause | Recommended actions |
|---|---|
| Overheating. | Check the thermocouple (powder control). |
| Contamination of residuals from lubricant of lower melting point. | Clean the slots with a cloth of linen textile at elevated temperature ( ~ 150°C) |

**Heat exchanger:** Powder leakage during deadlock.

| Cause | Recommended actions |
|---|---|
| The Slot Heater is out of line or the the slide valve doesn't close. | Adjust the Slot Heater to ensure that the slide valve is in a horizontal plane. |
| The powder leaks through the slide valve. | Control the slide valve at the heat exchanger in closed position. If still open, adjust the slide valve. |

**Heat exchanger:** Oil leakage at the oil heater during deadlock**.**

| Cause | Recommended actions |
|---|---|
| Failure of the nonreturn valve (between the oil heater and the hose). | Exchange the sealing ring inside the nonreturn valve. |
| The oil in the Slot Heater goes back into the oil tank and out through the overflow pipe. | |

## 10.2 Cone

**Cone:** No powder flow into the hose**.**

| Cause | Recommended actions |
|---|---|
| Overheating. | Check the thermocouple. Control the insulation material in the area where the thermocouple is placed. |
| | Replace if damaged; bad insulation cools down the thermocouple, which in turn could give overheating. |
| Overshoot in temperature due to powder left in the heating system.* | Close the valve and remove the powder left. Open the valve. |
| * The purpose of heating the cone is only in order to maintain the powder temperature, i.e. not to heat it up. | |

## 10.3 Hose

**Hose:** No powder flow into the filling shoe**.**

| Cause | Recommended actions |
|---|---|
| Overheating. | Check the thermocouple. Control the insulation material in the area where the thermocouple is placed. |
| | Replace if damaged; bad insulation cools down the thermocouple, which in turn could cause overheating. |
| Overshoot in temperature due to powder left in the cone at start-up of the heating system.* | Close the valve and remove the powder left. Open the valve. |
| Angle of hose between cone and the stationary feeder is not steep enough. (Recommended angle ≥ 65°.) | Change to a suitable length of hose. Increase the angle of the hose either by adjusting the distance between the Slot Heater and the press or the height between the Slot Heater and the stationary feeder. Change position of the stationary feeder. |
| * The purpose of heating the cone is only to maintain the powder temperature, i.e. not to heat it up. | |

## 10.4 Filling shoe

**Filling shoe:** Uneven temperature of the powder.

| Cause | Recommended actions |
|---|---|
| The cone filled up with a mixture of warm and “cold” powder due to powder leakage through slide valve. | Control the slide valve in the heat exchanger at closed position. If still open, adjust the slide valve. |
| | Ensure that the the Slot Heater is hanging so that the slide valve is in a horizontal plane. |
| Failure in the heating system (heat exchanger, cone, hose or filling shoe). | Control the temperature at the regulators and the resistance of the heating elements. |
| Insufficient insulation. | Control the condition of the insulation:<br>- Between the cone and the hose.<br>- Between the hose and the stationary filling shoe.<br>- At the stationary feeder.<br>- At the moving filling shoe. |
| Excess powder in the moving filling shoe compared to the rate of powder consumption required for the weight of the component. | Decrease the volume of the filling shoe by using an insert. |

**Filling shoe:** Arch formation.

| Cause | Recommended actions |
|---|---|
| Overheating as specified below: | |
| The heaters with a thermocouple between them are located inside the filling shoe, directly in contact. | Locate the heating elements and the thermocouple either outside the filling shoe (foil element) or in the walls of the filling shoe, i.e. cartridge heaters of same power and one of them with Built-in Thermocouple. |
| Due to misplaced thermocouple, e.g. too far distant from the heater. | Control the location. If the thermocouple is located more than 15-20 mm center distance to one of the heaters: change location. |
| Influence from the die (higher temperature) due to too long holding time on the die or too short distance between the stationary filling shoe and the die. | Insulate the adaptor table at the “loading station” from the die. If possible increase the distance between the stationary filling shoe and the die. |
| Too high temperature of the element located under the adaptor table. | Control the thermocouple and the insulation. |

## 10.5 Die

**Die:** Uneven temperature distribution.

| Cause | Recommended actions |
|---|---|
| Cartridge heater falling out due to large tolerances of the holes. | Control the tolerances of the holes. Install according to ISO F8. |
| Interruption on one of the heaters. | Control the electrical resistance. |
| Thermocouple misplaced. | Control the distance between the thermocouple and the heater, which should be no more than 15-20 mm center distance. |
| Insufficient number of cartridge heaters distributed or underpowered. | Calculate the power demand. Distribute the heaters evenly around the die. |

**Die:** Overheating.

| Cause | Recommended actions |
|---|---|
| The thermocouple has fallen out, which gives uncontrolled heating. | Control the location of the thermocouple. |
| Too much distance between thermocouple and heater. | Control the distance between the thermocouple and the heater, which should not be longer than 15 mm center distance. |
| Incorrect type of thermocouple. | Control that the thermocouple is of type “J”. In all the Slot Heaters manufactured by Linde the thermocouples in the whole heating system should be of type “J”, if nothing else is required. |

**Die:** The die insert popping out during compaction.

| Cause | Recommended actions |
|---|---|
| Insufficent shrink-fitting. | The shrink-fitting has to be adjusted to fit the operating temperature. |

**Die:** Scoring between die and punches or burr on the components.

| Cause | Recommended actions |
|---|---|
| Too tight clearance or too large clearance (powder in between punches and die). | The clearance has to be calculated to fit the operating temperature. |
| Too low temperature of the upper punch will give too large clearance. | Control the temperature of the upper punch. |

**Die:** High friction between adaptor plates and columns.

| Cause | Recommended actions |
|---|---|
| Variations in thermal expansion, due to higher temperature in the die plate as compared to rest of the adaptor plates. | Insulate the die from die plate by, e.g. water cooling, stainless steel materials, air-gap. |
| Not using heat resisting grease in the bearings (columns). | Exchange grease. |

## 10.6 Component

**Component:** Inconsistency in weight, height and density of compact.

| Cause | Recommended actions |
|---|---|
| Uneven temperature distribution in the powder. | See recommendations regarding the filling shoe. |
| Bad flowability of the powder due to overheating in the system. | Control the temperature in the heat exchanger, hose, filling shoe, adaptor table and die. |
| High friction between adaptor plates and columns. | See recommendations regarding the die. |
| Uneven feeding of the powder into the stationary feeder. | Control the angle of the hose between the cone and the stationary feeder. Recommended angle ≥ 65°. |
| Excess powder in the moving filling shoe compared to the rate of powder consumption required for the weight of the component. | Decrease the volume of the filling shoe by using an insert. |

**Component:** Lamination cracks in pressed components.

| Cause | Recommended actions |
|---|---|
| Insufficient design or condition of the die set. | Check the theoretical pore free density of the powder mix (see section 9.1). |
| Too high compaction force. | |

# 11 Gallery of warm compaction equipment

This section presents photography showing correct installation of warm compaction equipment. One possibility for adapting a tooling set to achieve robust heating is illustrated. The example pictured here is the tooling set used with a 400 ton Lauffer press at Höganäs. This unit has been installed according to the standards required for commercial production.

The press environment will always collect some loose dust from the iron powder supply. To protect the electrical system it is essential that all cables to the heating units are collected and covered with an insulating shield of glass fiber. Any exposed cable will be at risk of short-circuiting. **It is of upmost importance** that all parts connected to high currents be securely earthed.

To reduce set-up times, it is recommended that quick connecting sockets should be used. The number of loosely hanging cables at the rear of the press can be minimized with quick-coupling sockets as close as possible to the heating units. The connecting sockets for the die and upper punch could be positioned on the adaptor as shown in figures 48 and 51. The connecting sockets for the moving filling shoe and the adaptor table can be positioned as shown in the figure 54.

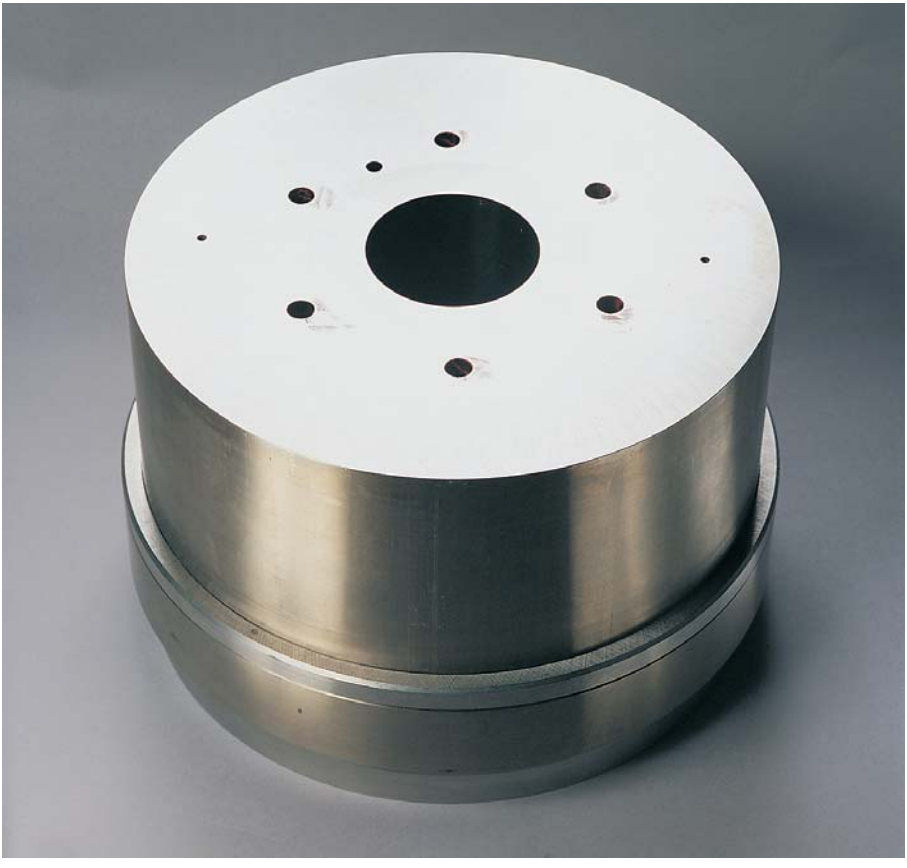

*Figure 45. Die, prepared for placement of heaters and thermocouple.*

*Figure 46. Heating accessories: cartridge heaters, thermocouple (center) and (at rear) a quick-coupling socket and section of insulating cover.*

*Figure 47. Cartridge heaters and thermocouple positioned in the die.*

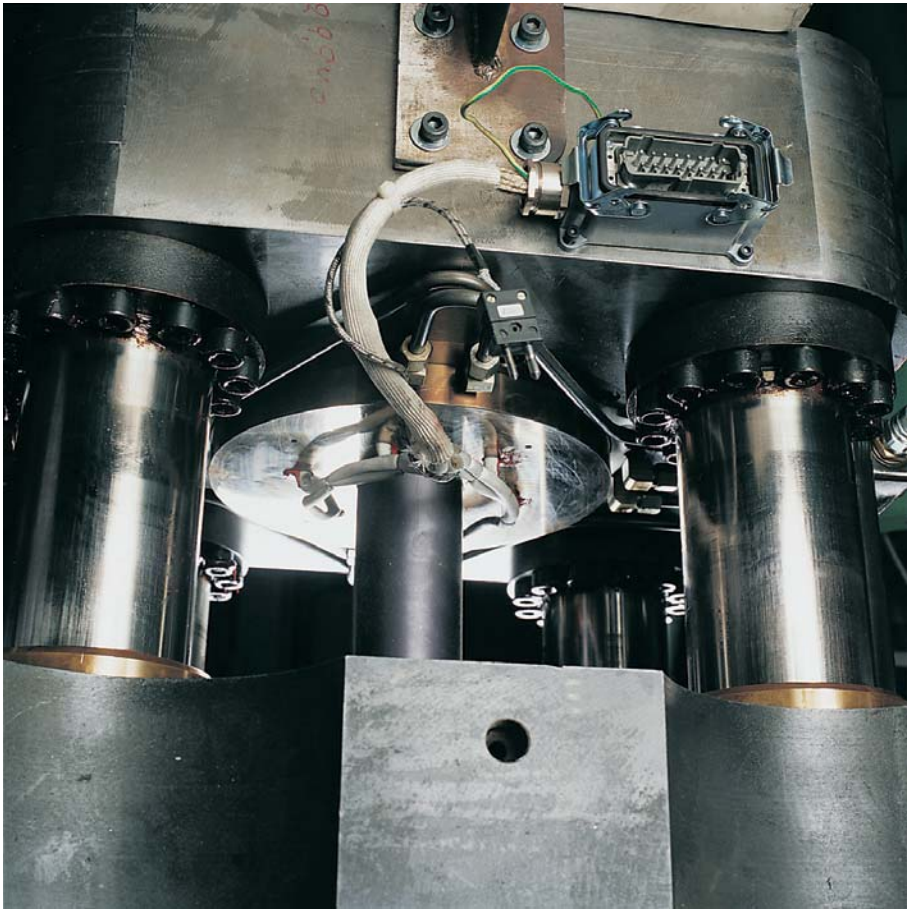

*Figure 48. Die fully mounted in the tool set with heating accessories connected to a socket for quick-coupling.*


*Figure 49. Upper punch and heating accessories (band heater, thermocouple and sockets).*

*Figure 50. Band heater and thermocouple positioned on the upper punch.*

*Figure 51. Upper punch fully mounted in tool set with heating accessories connected to a socket for quick-coupling.*

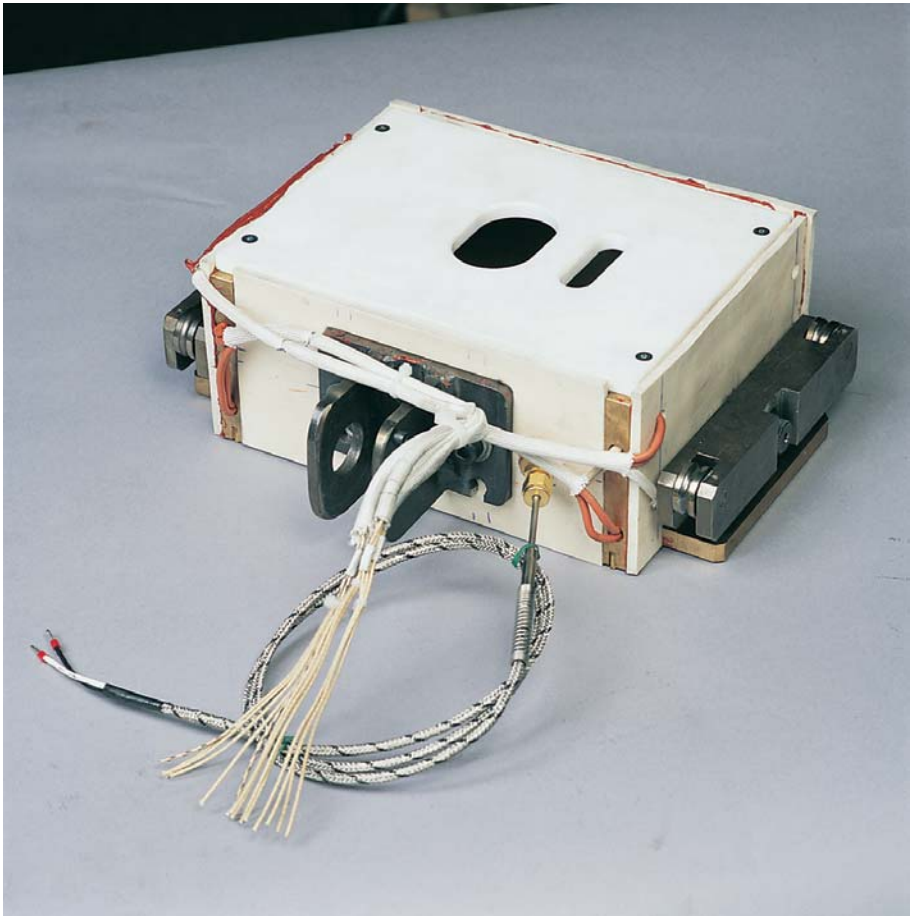

*Figure 52. Moving filling shoe equipped with heating accessories and insulation.*

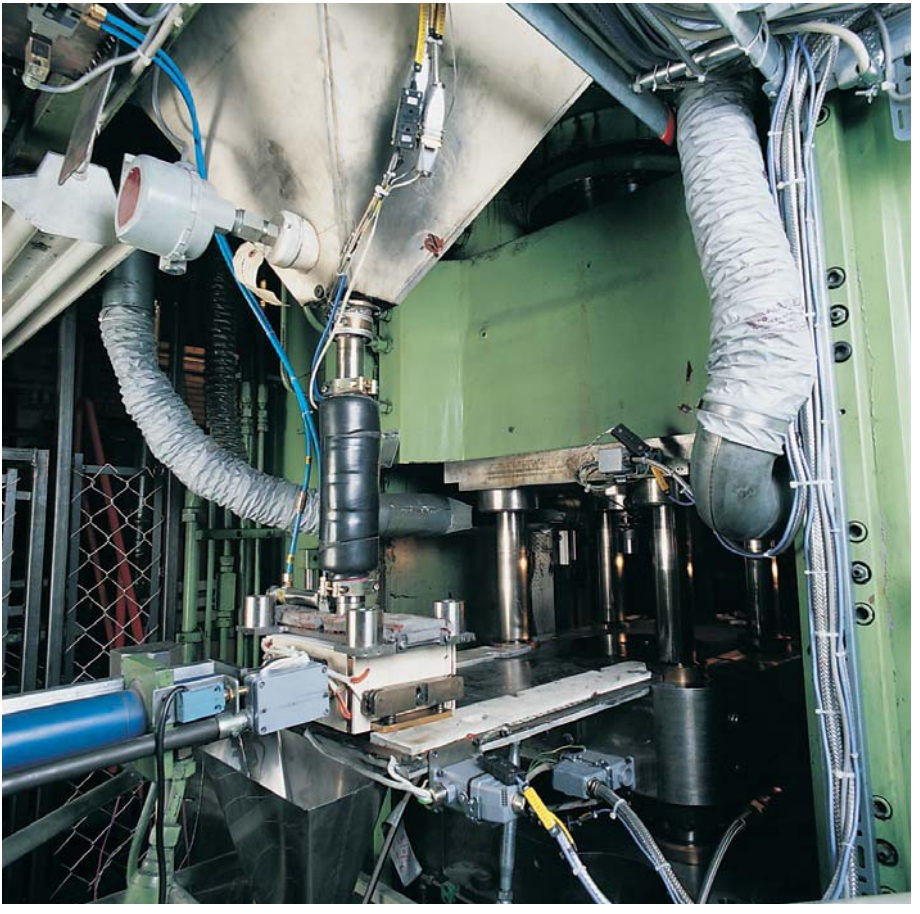

*Figure 53. Overview of filling system, including cone, hose, stationary feeder and the moving filling shoe in filling position.*

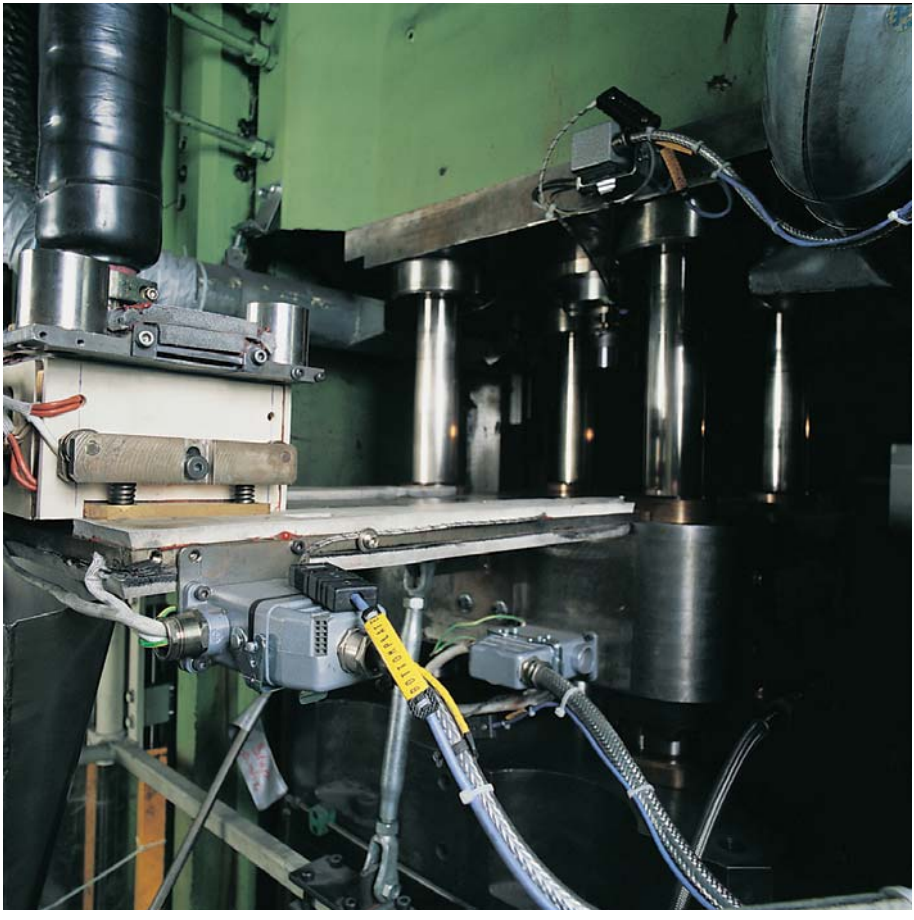

*Figure 54. Cable connections to the heating system of the moving filling shoe and adaptor table.*

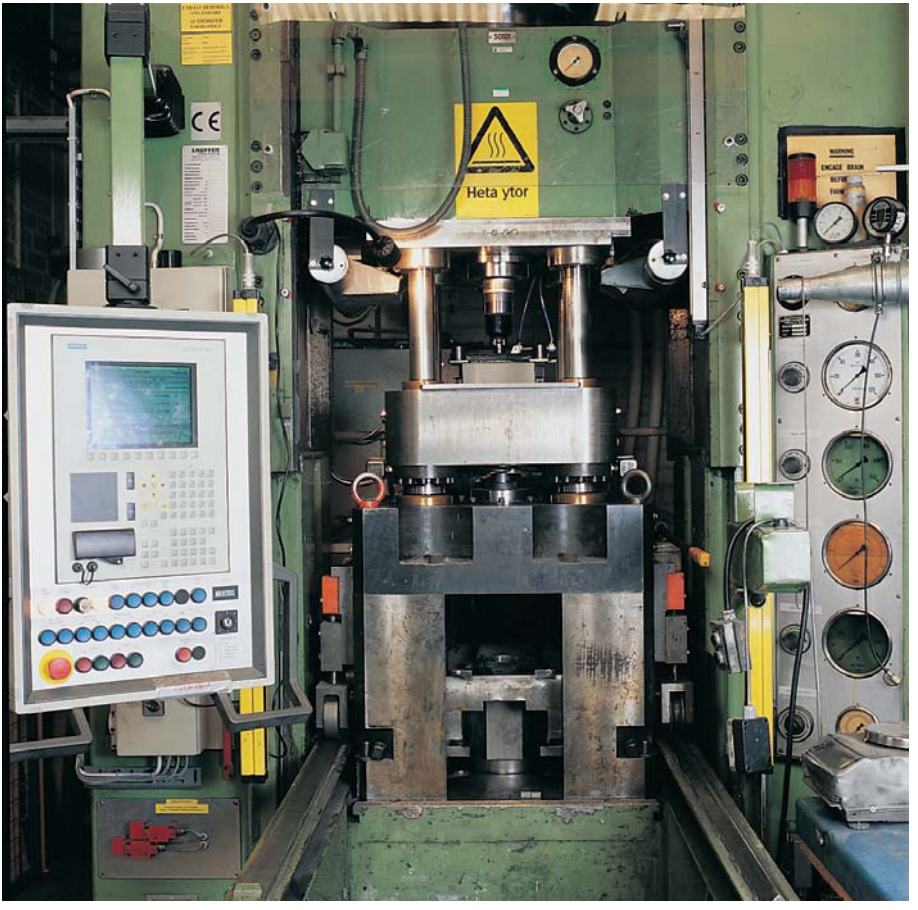


*Figure 55. Overview of the press, with the tool set in place.*

# 12 References


[1] U. Engström, B. Johansson & O. Jacobson. 'Properties and Tolerances of Warm Compacted PM Materials' Euro PM '95, Birmingham, 1995.

[2] B. Johansson, H. Rutz, F. Hanejko, S. Luk, & U. Engström. 'High Density PM Materials for Future Applications' Euro PM '94, Paris, 1994.

[3] J. Tengzelius. 'Höhere dichten durch Warmpressen' Symposium, Hagen, Germany, 1995.

[4] U. Engström & B. Johansson. 'Production Experience of Warm Compaction of Densmix Powders' PM2 TEC '96, Washington, 1996.

[5] O. Mårs. 'Dynamic Properties of Warm Compacted High Strength Steels' PM2 TEC '96, Washington, 1996.

[6] H. Rutz, F. Hanejko & S. Luk. 'Warm Compaction Offers High Density at Low Cost' Metal Powder Report, Vol. 49, No. 9, Elsevier Advanced Technology, Oxford, 1994.

[7] W. M. Long. Powder Metallurgy, No. 6, 1960.

[8] G. Bockstiegel. Unpublished data held by Höganäs AB, Sweden, 1967.

[9] G. Bockstiegel & J. Hewing 'Verformungsarbeit, Verfestigung und Seitendruck beim Pressen von Metallpulvern' Zweite (Nu. 2) Europäisches Symposium über Pulvermetallurgie, Stuttgart, Germany, 1968.

[10] G. Bockstiegel. Example: the yield point s0(T) decreases with increasing temperature. T (T3>T2>T1). Unpublished paper held by Höganäs AB, Sweden, 1967.

[11] J. M. Capus. 'Pushing the Limits of Densification' Metal Powder Report, July/ August, 1995.

[12] G. E. Dieter. Mechanical Metallurgy, 3rd ed. (SI Metric Edition), McGraw-Hill (UK), 1988.

[13] J. Tengzelius .'Challenges for the Iron Powder Industry in the Next Millennium' Euro PM '97, München, Germany, October, 1997.

[14] M. Larsson & J. Rassmus. 'Higher Tolerances by Improved Materials and Processes' PM '98 World Congress, Granada, Spain, 1998.

[15] P. G. Arbstedt, Metals Technology, May-June, 1976.

[16] U. Engström, B. Johansson & J. Rassmus, 'Porosity and Properties of Warm Compacted High Strength Sintered Steels' PM '98 World Congress, Granada, Spain, 1998.

[17] M. Johansson & M. Strömgren. 'Sätt och anordning för uppvärmning av pulver samt användning av anordningen' Swedish patent SE 502701.

[18] D. R. Gaskell. Transport Phenomena in Materials Engineering, Macmillan Publishing, (USA) 1992.

[19] B. W. Goe & R. C. Hertlein. 'Auger conveyor assembly for heating and feeding polymer coated powder to the shuttle of a compacting press' US patent 5593707.

[20] G. F. Bocchini. Warm Compaction of Metal Powders: Why it works and why it requires a sophisticated engineering approach . Unpublished paper held at Höganäs AB, Sweden.

[21] G. F. Bocchini. 'Friction effects in metal powder compaction: Part 1 - Theoretical aspects' International Conference on P/M and Particulate Materials, Seattle, May 14-17, 1995.

[22] G. F. Bocchini, R. Esposito & G. Cricri. 'Influence of operating temperature on shrink fitting pressure of PM dies', Powder Metallurgy, Vol. 39, No. 3, pp. 195-206, 1996.

[23] R. Köller & J. Massinger. Unpublished data held at IFAM, Bremen, Germany, 1997.

[24] ISO 3252 'Withdrawal tool set' (International Standards Organization).